CHALMERS
UNIVERSITY OF TECHNOLOGY

Development of manganese ore as oxygen carrier for CLC and CLOU

Report for Master's thesis in Materials Chemistry
Mainly performed at Tsinghua University, Department of Thermal Engineering

Andreas Viggeborn

Chemistry and Chemical Engineering, Environmental Inorganic Chemistry
CHALMERS UNIVERSITY OF TECHNOLOGY
Gothenburg, Sweden 2019

Master's thesis 2019:KBTX12

Development of manganese ore as oxygen carrier for CLC and CLOU

Andreas Viggeborn

CHALMERS
UNIVERSITY OF TECHNOLOGY

Environmental Inorganic Chemistry
Chalmers University of Technology
Gothenburg, Sweden 2019

Development of manganese ore as oxygen carrier for CLC and CLOU

A master thesis mainly performed at Tsinghua University in Beijing, China

© Andreas Viggeborn, 2019.

Supervisor: Zhenshan Li, Department of Thermal Engineering
Examiner: Henrik Leion, Department of Environmental Inorganic Chemistry

Master's Thesis 2019:KBTX12
Department of Environmental Inorganic Chemistry
Chemistry and Biochemistry
Chalmers University of Technology
SE-412 96 Gothenburg
Telephone +46 31 772 1000

Typeset in LaTeX
Printed by Chalmers Reproservice
Gothenburg, Sweden 2019

Development of manganese ore as oxygen carrier for CLC and CLOU
ANDREAS VIGGEBORN
Chemistry and Chemical Engineering, Environmental Inorganic Chemistry
Chalmers University of Technology

Abstract

Production of electricity and heat is a large source of greenhouse gas emissions, mainly carbon dioxide, which is believed to cause climate change. Methods to reduce the carbon dioxide emissions by capturing and storing it are being the focus for research, one of these methods is the chemical looping-combustion (CLC). One vital component of the CLC process is the oxygen carrier.

This thesis tried to develop oxygen carriers based on manganese ores using two different manganese ores originating from China. Kaolin, a mineral, was added to the ores in order to improve the physical strength of the particles as well as increasing the melting point. These improvements were done to decrease attrition and reduce the risk of agglomeration. Crushing tests and a novel optical image method were performed to evaluate these properties. The addition of kaolin decreased the CLOU properties and the reactivity to convert fuel. To reduce this negative effect impregnation of the oxygen carriers were done using $Cu(NO_3)_2$ and $Ca(OH)_2$. Two different types of TGA were done to investigate the change in CLOU properties. Additional TGA tests were done with different temperature setups to investigate the performance of the oxygen carriers for application in a future CLC process.

The addition of kaolin improved the mechanical strength of all particles as well as increased the melting temperature. The impregnation with calcium did prove ineffective but the copper impregnation improved the CLOU properties. The copper impregnation did lower the melting temperature of the particles. An oxygen carrier was manufactured with kaolin as an additive and later impregnated with copper that showed similar reactivity while having better physical properties than a nontreated oxygen carrier from the same manganese ore.

Keywords: oxygen carrier, manganese ore, kaolin, impregnation, copper, CLC, CLOU.

Acknowledgments

I would like to thank Henrik Leion and Zhenshan Li for providing me with this opportunity to perform this master thesis at Tsinghua University. I would also like to thank them for always being supportive and taking their time if I ever needed help with anything. A big thank you to Åforsk for providing economic funding which helped facilitate this exchange. Last but not least I would like to express my greatest appreciation to Lei Liu for supporting me during this project but also for making me feel at home in Beijing.

Andreas Viggeborn, Beijing, June 2019

Contents

1 Introduction **1**
1.1 Carbon capture-techniques . . . 1
1.1.1 Conventional carbon capture techniques . . . 1
1.1.2 Chemical looping-combustion . . . 2
1.1.3 Alternative applications . . . 3
1.2 Oxygen Carriers . . . 4
1.2.1 Mn-based oxygen carriers . . . 4
1.2.1.1 Synthesized oxygen carriers . . . 5
1.2.1.2 Ore-based oxygen carriers . . . 5
1.2.2 Stabilizers . . . 7
1.2.3 Impregnation . . . 8
1.3 Aim . . . 8

2 Experimental section **9**
2.1 Oxygen carrier preparation . . . 9
2.1.1 Impregnation . . . 10
2.2 Crushing test . . . 11
2.3 TGA . . . 11
2.3.1 Regular TGA . . . 11
2.3.2 Macro TGA . . . 12
2.4 Melting characteristics . . . 12
2.5 Data evaluation . . . 14
2.5.1 Regular TGA . . . 14
2.5.2 Macro TGA . . . 15
2.5.3 Kinetic model . . . 15

3 Results **16**
3.1 Crushing test . . . 16
3.2 Regular TGA . . . 16
3.2.1 Addition of kaolin . . . 16
3.2.2 Impregnation . . . 18
3.2.2.1 Copper . . . 18
3.2.2.2 Calcium . . . 19
3.2.3 Post redox tests . . . 20
3.2.4 Temperature investigation . . . 22
3.2.5 Kinetic model . . . 23

3.3 Macro TGA 25
3.3.1 Addition of kaolin 25
3.3.2 Impregnation 26
3.4 Melting characteristics 27

4 Discussion **29**

5 Conclusion **32**

A Appendix 1 **I**
A.1 TGA experiments I
A.1.1 FJ with kaolin I
A.1.2 LY with kaolin III
A.1.3 FJ with copper impregnation VII
A.1.4 LY with copper impregnation IX
A.1.5 Post macro TGA XI
A.1.6 Temperature investigation XV

1
Introduction

The climate changes we are seeing are most likely the consequences of an increasing amount of greenhouse gas in the atmosphere and CO_2 is one of these greenhouse gases [1]. In 2016, 25% of the global emissions of greenhouse gas originated from electricity and heat production and a large part of this was CO_2 from power plants that burned fossil fuels to produce energy [1].

1.1 Carbon capture-techniques

To decrease emissions, different techniques for carbon capture which can be implemented at plants are being investigated and developed. Pre-combustion, post-combustion and oxyfuel combustion are examples of conventional carbon capture techniques [2]. What these techniques have in common is the aim to separate the CO_2 from the other combustion products. The purified CO_2 can later be pressurized and stored in for example depleted oil fields or saline aquifers and thereby decreasing the amount of CO_2 emissions released into the atmosphere [2, 3]. An investigation made by Kanniche et al. concluded that due to their different designs and consequently different advantages it was not possible to declare one method as better than the others [4]. These three methods are briefly described below.

1.1.1 Conventional carbon capture techniques

The first step in the pre-combustion method is the conversion of the fuel into synthetic gas (syngas), which consists mainly of H_2 and CO [5]. The following step requires a catalytic reactor where the CO is converted into CO_2 and after the conversion, a separation of H_2 and CO_2 is necessary [5]. Post-combustion separates the CO_2 from the flue gases, such as N_2 and unreacted O_2 through a gas-gas separation after the combustion [2]. Separating through amine absorption is used today in other gas absorption applications but studies showed that applied on CO_2 capture it would decrease the energy output of the plant's by about 30% to capture 90% of the CO_2 [6]. Laboratory tests with membranes done by Merkel et al. indicated that 90% CO_2 could be capture while consuming 16% of the plants original energy output [6].

In oxyfuel combustion almost pure oxygen (usually >95% O_2) is used which is produced from regular air [7]. During combustion, most of the oxygen is consumed and the flue gas will consist of mainly CO_2 and H_2O which does not require as much

energy to separate, for example CO_2 and N_2 and the purified CO_2 can be stored [7]. The major drawback with this method is that purifying oxygen from the air is energy demanding, reducing the overall efficiency of the process and if NO_x and SO_x gas are produced during the combustion it would contaminate the CO_2, possibly leading to further separation [7]. In addition to previously mentioned issues, pilot studies have revealed issues with the stability of the combustion for this process design [7]. Because these three methods all have the drawback of being energy and/or material demanding none of them are attractive as of now [2].

1.1.2 Chemical looping-combustion

One alternative to previously mentioned carbon capture techniques is the chemical looping-combustion (CLC). By supplying the oxygen needed for the combustion with the help of a solid material, called an oxygen carrier , the process can separate the fuel from the oxygen source using two different reactors, the fuel reactor and the air reactor [8]. The oxygen carrier is cycled between the two reactors and is reduced in the fuel tank and oxidized in the air reactor, as shown in Figure 1.1. Because of the separation of the air and the fuel, the gas flow out of the air reactor consists of unreacted O_2 and N_2 while the gas flow out from the fuel reactor mainly consists of CO_2 and H_2O, thereby avoiding the costly gas-separation of CO_2, O_2 and N_2, a clear advantage compared to previously mentioned carbon capture methods.

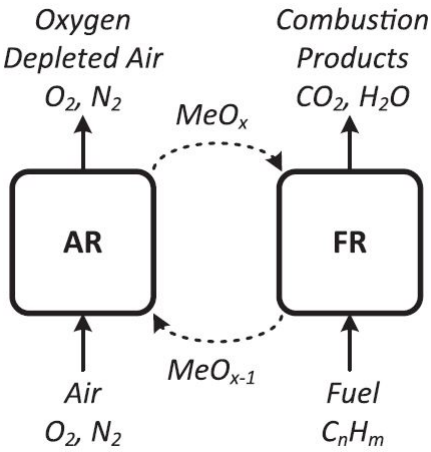

Figure 1.1: A schematic overview of the chemical looping-combustion process [9].

There are several subcategories of the CLC process, such as ex-situ gasification CLC (eG-CLC) and in-situ gasification (iG-CLC). Both eG-CLC and iG-CLC involves solid fuel with the difference that in eG-CLC the fuel is gasified to syngas before the CLC process and in iG-CLC, the solid fuel is fed into the fuel reactor where it is gasified and combusted [10]. Another variation is chemical-looping with oxygen uncoupling (CLOU) where the metal oxide releases oxygen, often through a phase transition [9]. The equilibrium reaction between the oxygen carrier and the oxygen, described in equation 1.1, depends on the partial pressure of oxygen. The partial

pressure depends in turn on the temperature and pressure and the equilibrium point differs from material to material [9].

$$\mathrm{MeO_x}(s) \rightleftharpoons \mathrm{MeO_{x-1}}(s) + \frac{1}{2}\,\mathrm{O_2}(g) \tag{1.1}$$

The CLC process relies heavily on the performance of the oxygen carrier which explains the large interest and funding in the field of oxygen carrier research. For a material to fit as an oxygen carrier, it needs to fulfill certain criteria. It needs to have good reactivity with the fuel in order to fully convert it [8]. It also needs to have good mechanical strength because of the impacts with other particles or the reactor walls that they experience. An oxygen carrier with low mechanical strength would result in large attrition leading to a low lifetime of the oxygen carrier and to maintain the conversion more material would need to be added, increasing the cost. If the particles would agglomerate it would impair and in the worst case completely stop the fludization, thus good fluidization properties are an important property to keep this from happening. The oxygen carrier should also be cheap since there is a loss of oxygen carrier through the attrition previously mentioned but also while removing fuel residues from solid fuels such as ash. Being environmental friendly would also simplify potential waste disposal [11].

There are several CLC pilot plants around the world of different sizes. To name a few, Chalmers University of Technology has a 10kW and a 100kW, Tsinghua University has a 30kW, a 120kW plant is located at TU Wien and TU Darmstadt has a 1MW plant. Tsinghua University, however, is in the progress of building a 3MW plant which is expected to be finished in early 2022. Modeling and simulations of CLC plants have also been done, ranging from smaller plants up to 1000MW. In a modeling of a 10 MW CLC demonstration plant, the boiler performance was very high considering CO_2 was also being captured [12] and the study of a 1000 MW plant concluded that the price for capturing 1 tonne of CO_2 would be €20 [13].

1.1.3 Alternative applications

Besides being a key component of the CLC process oxygen carriers can be used in other applications such as Oxygen Carrier Aided Combustion (OCAC) and chemical-looping partial oxidation of methane. OCAC uses a typical fluidized bed reactor but some or all of the inert fluidization material (often silica sand) is substituted with an oxygen carrier [14]. The oxygen carrier will be oxidized in oxygen-rich sections and reduced in fuel-rich sections [14]. Experiments executed in a 12 MW-boiler at Chalmers University of Technology showed that with parts of the inert bed material replaced by a manganese ore as an oxygen carrier, the oxygen demand could be lowered substantially without increasing the emission of CO [15]. Historically, partial oxidizing of methane to syngas can be done either with steam reforming or by using noble metals (eg. Pd, Rh and Ru) as catalysts at high temperature. But since using steam is energy demanding and noble metals are expensive, an alternative solution with chemical-looping of oxygen carriers has gained interest [16]. Methane is partly oxidized in the fuel reactor by the oxygen carrier which is then cycled to the air reactor where it is re-oxidized.

1.2 Oxygen Carriers

Due to their good redox ability metal oxides have been the most common choice when investigating materials for oxygen carriers. The most investigated oxygen carriers have been oxides based on Cu, Fe, Ni and Mn, and both monometallic and combined metal oxides have been investigated. Figure 1.2 shows the average price for different raw materials used for oxygen carriers with Fe and Mn having a substantially lower price than Cu and Ni.

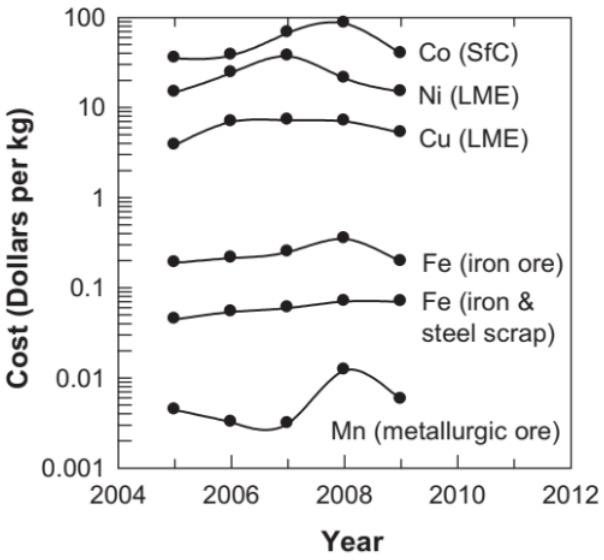

Figure 1.2: Cost for raw materials used for the production of oxygen carriers [17].

Ni was tested early on with good results, showing good reactivity with a full conversion as a result and low attrition on the particles [18, 19, 20]. A major drawback for nickel is the high price and toxicity and therefore other alternatives were sought after [21]. Several studies have shown that Cu based oxygen carriers have good reactivity with both syngas and solid fuels [22, 23, 24]. They have however also shown a tendency to agglomerate and possibly terminating the fluidization [25, 26]. This is mainly attributed to the relatively low melting point of metallic Cu which is 1085 °C[17], Ni for example has a melting point of 1454°C. Cu is relatively expensive but it is environmentally friendly and it has shown to have CLOU properties [27]. Fe-based oxygen carriers are cheap, the raw materials are abundant and it is environmentally friendly [17]. Compared to other oxygen carrier materials the reactivity is quite poor but due to the low price, it is still an interesting option [28].

1.2.1 Mn-based oxygen carriers

The main benefit of using manganese as raw material is the low price, the environmentally character while still having an acceptable reactivity towards the fuel. Another benefit is the shown CLOU properties, which could improve reactivity with

solid fuel as in iG-CLC [27].

Manganese can exist in several different oxide states but the one considered relevant for CLC applications is the transformation between Mn_3O_4 and MnO [17]. Monometallic Mn-based oxygen carriers were tested early but did not produce convincing results. When several monometallic oxides were tested for combustion of coal Mn_2O_3 performed worse than CuO, NiO, Fe_2O_3 and Co_3O_4 [23] and MnO_2 was outperformed by both CuO and Fe_2O_3 when methane was used as fuel [29].

1.2.1.1 Synthesized oxygen carriers

A large number of combined metal oxides have been synthesized and tested with manganese as one of the components. It has been tested in combination with Fe, Mg, Ca, Al and Si with different compositions and sometimes with more than one element. Schmitz et al. produced an oxygen carrier from Mn_3O_4, TiO_2 and SiO_2 through spray-drying [30]. It demonstrated good reactivity in a 10 kW CLC pilot unit and the lifetime was roughly estimated to 2900-5600 hours. Adánez-Rubio et al. synthesized an oxygen carrier based on CuO and Mn_3O_4 using spray granulation [31]. It performed well conversion wise with coal as fuel in a 1.5 kW CLC unit but the attrition was slightly higher than what has previously suggested as tolerable levels. It was believed that some of the attrition was a result of chemical stress that the oxygen carrier received during the operation. Mn_3O_4, Fe_2O_3 and TiO_2 with different Mn/(Mn+Fe) ratios were synthesized by Abián et al. through sintering of pellets consisting of the three oxides which were later crushed to obtain particles of suitable size [32]. The particles had a crushing strength of 4-5N, an increase from 2-3N, which was attributed to the titanium. Reactivity of the particles were tested with CH4, CO and H2 and particles with a Mn:Fe:Ti ratio of 80:13:7 had the best reactivity. Particles which consisted of 0.5-0.8 mass ratio manganese showed clear oxygen uncoupling properties.

Synthesized oxygen carriers have in general shown good performance with good reactivity and high durability. Their biggest drawback however is the price of the manganese oxide used as raw material to manufacture them. The high price makes it unattractive for large scale operation and scaling up production from lab scale to industrial scale can be coupled with high costs.

1.2.1.2 Ore-based oxygen carriers

Despite that many synthesized oxygen carriers have been successfully manufactured and showed promising performance in small scale tests, the disadvantages have led to other alternatives being investigated. Many trials have been made with oxygen carriers made out of natural occurring ore or mineral waste products. The main reason for this is the lower cost of a mineral-based oxygen carrier compared to a synthesized due to raw materials being available in large quantities.

An oxygen carrier made from mineral waste from Colombia was analyzed by Velasco-Sarria et al. [33]. Thermal treatment of the particles increased the crushing strength to 3N, an increase of 29%. To test its reactivity the particles were put through 50 redox cycles in a bench-scale batch fluidized reactor with CO, H_2 and CH_4 used as fuel. It performed better than ilmenite, a low-cost iron mineral, oxygen carrier with the three gaseous fuels tested and in later tests it performed better with CO, equally good with CH_4 but slightly worse with H_2 when compared to an oxygen carrier made out of manganese minerals. While it was not tested in a real CLC process it did have an air jet attrition index below 5 which suggests a lifetime of above 2000 hours. Another study that also evaluated the suitability of manganese ores was Leion et al. [34]. Redox cycles of seven different manganese oxygen carriers was conducted along with crushing strength tests. The reactivity of the seven manganese-based oxygen carriers was concluded as good but they had poor mechanical properties. Only two had a crushing strength above 1N and five of them showed poor fluidization properties, only one showed good fluidization performance and had an acceptable crushing strength.

Moldenhauer et al. compared a synthesized Mn:Fe:Al oxygen carrier with a ratio of 1:2:0.64 to an ore-based one called Metmin which were both tested in a 300W bench-scale CLC setup [35]. Metmin showed the highest amount of oxygen uncoupling in an earlier big screening of ore-based oxygen carriers but did suffer from high attrition and had a lower reactivity than most other oxygen carriers tested in the screening, all of which were based on manganese ores [36]. During the experiments by Moldenhauer et al. both oxygen carriers showed CLOU properties with the ore-based releasing a slightly higher amount of oxygen. In order to achieve above 99% conversion of syngas 45% more Metmin oxygen carrier than the synthesized oxygen carrier needed to be used in the process. Another difference between the two was that Metmin had a higher conversion with methane but a slightly lower conversion of kerosene and syngas. Both oxygen carriers operated for more than 20 hours and the synthesized oxygen carrier produced less fines which should indicate a longer lifetime but no lifetime was approximated.

Three different manganese ores were tested by Schmitz et al. in a 10 kW CLC pilot plant at Chalmers University of Technology[37]. Two of them, named Mesa and Mangagran, were based on manganese ore while the third one called Sinfin was a material derived from manganese ore handling. They were all sintered at 950 °C for 24 hours. The Mesa and Sinfin did suffer from mild agglomeration during the sintering which was easily broken apart afterward. All manganese oxygen carriers performed better than an ilmenite-based oxygen carrier which was previously tested in the same pilot plant with pet-coke as fuel. Due to agglomerations during operations the Mesa material was ruled out as an oxygen carrier candidate. The calculated lifetime on Sinfin and Mangagran was 284h and 109 hours respectively. Comparatively, ilmenite-oxygen carrier tests done in a 100 kW plant also at Chalmers had an estimated lifetime of 700-800 [38].

Linderholm et al. tested an oxygen carrier, named Sinaus, made from Australian

manganese ore in a 100 kW pilot CLC process ore with different fuels for a total run time of around 50 hours [39]. With pet-coke, Sinaus had the same conversion (95%) as an ilmenite ore had previously in the same pilot process but Sinaus achieved a higher degree of carbon capture. Furthermore, the conversion of coal with Sinaus was the highest achieved in this pilot facility so far. The lifetime was approximated to 100-400h, significantly lower than other manganese ore based oxygen carriers. It should be noted that many other studies have estimated the lifetime using jet cup tests while Linderholm et al. estimated it from the loss of fines during the CLC operation.

Another experiment with a Brazilian manganese ore oxygen carrier was done by Berdugo Vilches et al. [40]. They performed lengthy tests in a process of semi-industrial scale with conditions similar to a CLC process, accumulating more than 1000h in total. The gasifier which resembles the fuel reactor was 2-4 MW and biomass was used as fuel. The manganese ore had a larger oxygen demand than the ilmenite did and therefore issues with reactivity. During these tests, the manganese oxygen carrier was out-performed by the ilmenite based oxygen carrier in regards to reactivity. This result does contradict some of the previous research where manganese-based ores have performed better than ilmenite. Differences between this experiment and earlier were longer run time and that biomass was used as fuel which could be the reason behind ilmenite outperforming the manganese ore. While attrition was not mentioned as an issue it should be noted that the fluidized bed was only mildly fluidized which would probably increase the lifetime of the particles compared to a normal CLC process.

1.2.2 Stabilizers

Experiments have been done by Haider et al. to improve the mechanical properties of copper oxide with an alumina rich cement [41]. The copper oxide and the alumina-based cement were ground and mixed for 24 hours in a ball mill. Water was then sprayed during the mixing of the powder until particles were of the wanted size. Around 150-200 mL of water was added to 1 kg of the mixture and the resulting particles were later air-dried at 200°C. The final step was the sintering of the particles at 900°C for 4 hours before being sieved in order to receive particles of suiting size. The crushing strength for pure copper oxide used in the experiment was on average 0.43N and with the added alumina it increased to 1.23, 1.27 and 1.55 for 25, 50 and 75 wt% alumina cement respectively. The particles with 25 and 50 wt% cement experienced agglomeration but not the particles manufactured from 75 wt% cement. Copper has as previously mentioned suffered from agglomeration issues mainly due to its lower melting point. The reactivity with CO was tested through 25 redox cycles and showed that samples with more copper oxide had better conversion and also that the conversion was the highest during the first redox cycle. At the time no successful trials have been made to improve the mechanical properties of manganese ore-based oxygen carrier by addition of stabilizers, but the trials by Haider et al. demonstrated a possible method for improving the mechanical properties.

1.2.3 Impregnation

It has previously been demonstrated that the reactivity of manganese ores as oxygen carriers can be increased by impregnating it with copper. During a study by Xu et al. wet impregnation was performed with copper nitrate solutions on three manganese ores [42]. Both impregnating with 0.5 and 2 wt% improved the reactivity, impregnating with 10 wt% did not show better reactivity than the sample with 2 wt% as well as tendencies to agglomerate so it was suggested that the impregnation should be kept under 2 wt%. Another study also done by Xu et al. tested copper impregnation on several different manganese ores and saw that the reactivity increased for all of them and it seemed to have the biggest effect on ores that had a low reactivity from the beginning [43].

1.3 Aim

Many studies have been conducted to investigate the performance of oxygen carriers based on manganese ore but few have tried to improve their properties. A big drawback with manganese ore-based oxygen carriers is its mechanical properties which result in a low lifetime when used in a CLC process. An improved lifetime would lower the overall cost for carbon capture making the CLC process more attractive for commercial use. One documented way of improving the mechanical properties of an oxygen carrier is with alumina rich cement which was done with a copper-based oxygen carrier. Kaolin is a mineral rich with aluminum and it is cheap and available at a large quantity enabling an inexpensive oxygen carrier. The aim of this master's thesis is to improve the mechanical properties of oxygen carriers based on two Chinese manganese ore by adding kaolin. Improved crushing strength should increase its lifetime and a higher melting point should reduce the risk of agglomeration. One drawback of adding kaolin is that the CLOU properties and the reactivity of the oxygen carrier could potentially be lowered. To counter this a copper impregnation will be done through a wet impregnation. The aim is that the new method will result in an oxygen carrier with improved lifetime and sustained or even improved reactivity.

2
Experimental section

This section describes the preparation steps of the oxygen carriers and the different experiments performed to evaluate the manufactured oxygen carriers.

2.1 Oxygen carrier preparation

The oxygen carriers evaluated were based on one of two different types of natural manganese ores, called LY and FJ. Both ores have their origins in China where the LY ore had been mined near the city of Leiyang which is located in the Hunan province and FJ was mined in the Fujian Province. The elemental compositions of the two ores had previously been analyzed with X-ray fluorescence and the results are presented in Figure 2.1. A few distinct differences in composition were that the LY ore had a higher manganese content, a slightly lower iron content and a much lower potassium content than FJ has.

Mn Ore: LY

Element	Wt%	Est.Error
Mn	48.57	.22
Fe	8.29	.11
Si	4.77	.16
Al	.832	.07
Na	1.14	.07
K	.618	.025
P	.323	.016
Mg	.274	.030
Ti	.169	.0094
Ba	.222	.024
Ca	.157	.0091
V	.0546	.0027
Sr	.0741	.0037
Zn	.0183	.0012
Zr	.0108	.0026
W	.0114	.0036
Pb	.0121	.0036
Bi	.0100	.0021
Cr	.0074	.0012

Mn Ore: FJ

Element	Wt%	Est.Error
Mn	38.11	.14
Fe	10.08	.12
K	9.45	.11
Si	3.63	.14
Al	1.81	.11
Ca	.890	.05
Na	.895	.06
P	.240	.012
Mg	.223	.025
Ba	.284	.017
Ti	.165	.0092
Zn	.0854	.0043
Sr	.0823	.0041
Ni	.0352	.0053
S	.0129	.0006
V	.0164	.0009
Pb	.0194	.0020
Zr	.0111	.0015
Bi	.0101	.0013

Figure 2.1: Analysis of the elemental composition in terms of wt% using XRF. The values to the left are from the LY ore and the right are the FJ ore.

To prepare the oxygen carriers the ore powders were mixed with different amounts of kaolin and organic binder. The kaolin was purchased from Sinopharm Chemical Reagent Co., Ltd. and had a purity of 99.38%. In this study, mixtures with 5, 10 or 15 dry wt% were tested and compared to oxygen carriers with no added kaolin.

Dextrin was used as the organic binder which was also bought from Sinopharm Chemical Reagent Co. Ltd. Roughly 100mg binder was dissolved per 1L water and added to the powder through spraying while mixing it. Water and binder solution was added until the powder formed small lumps with roughly 0.5-2.5 cm in diameter. The agglomerated particles were sintered for 8 hours at mainly 1100 °C with one exception that was sintered at 950 °C. After being calcined the now hard particles were crushed to a fine powder and sieved to get particles in the size range of 150-300 microns. The 18 different oxygen carriers that were manufactured and tested are summarised in Table 2.1 below.

Table 2.1: Summary of the different compositions of oxygen carriers that were manufactured and tested.

Label	Ore	Sintering Temperature[C]	Kaolin [wt%]	Cu/Ca [wt%]
FJ-Mn0-950	FJ	950	0	0
FJ-Mn0-1100	FJ	1100	0	0
FJ-Mn5-1100	FJ	1100	5	0
FJ-Mn10-1100	FJ	1100	10	0
FJ-Mn5-1100-Cu0.5	FJ	1100	5	0.5
FJ-Mn5-1100-Cu2	FJ	1100	5	2
FJ-Mn5-1100-Cu5	FJ	1100	5	5
FJ-Mn5-1100-Blank	FJ	1100	5	0
FJ-Mn5-1100-Ca0.5	FJ	1100	5	0.5
FJ-Mn5-1100-Ca2	FJ	1100	5	2
FJ-Mn5-1100-Ca5	FJ	1100	5	5
LY-Mn0-1100	LY	1100	0	0
LY-Mn5-1100	LY	1100	5	0
LY-Mn10-1100	LY	1100	10	0
LY-Mn15-1100	LY	1100	15	0
LY-Mn5-1100-Cu0.5	LY	1100	5	0.5
LY-Mn5-1100-Cu2	LY	1100	5	2
LY-Mn5-1100-Cu5	LY	1100	5	5

2.1.1 Impregnation

The manganese ores were impregnated with either copper or calcium through a wet impregnation method. The oxygen carrier with 5 wt% kaolin was chosen for further evaluation with impregnation after the initial TGA tests. Roughly 10 g of Mn5-powder was mixed with either $Cu(NO_3)_2$ or $Ca(OH)_2$ powder and dissolved in approximately 75 mL deionized water and left for 10 hours to soak. After the soaking period, they were dried in an oven for six hours at 500 °C. One sample that was not impregnated was also in the oven for six hours and is called FJ-Mn5-1100-Blank. Three different amounts of salt were added and they indicate the dry wt%

of the wanted ion, in this case, Cu and Ca. As an example, this meant that the FJ-Mn5-1100-Cu2 dry mixture had 2 wt% of Cu before being soaked in water.

2.2 Crushing test

In order to test the mechanical strength of the oxygen carrier particles, crushing strength tests were performed. The test consists of testing how large the force is that is needed to break a single particle that was 100 microns large slightly bigger and a total of 10 particles were evaluated for each to get an average value. The instrument used was a WDW 3020. Particles with added kaolin or no kaolin was tested however no impregnated particles were tested. The reason for this was that it proved difficult to find particles of the right size to test.

2.3 TGA

Thermal gravimetric analysis (TGA) experiments were performed to evaluate the CLOU properties of the samples and the reactivity with H_2. During the experiment, the weight change of the sample over time is measured while controlling the temperature. In this case it can be used to determine to what extent the sample can release and take up oxygen in different atmospheres. Two different TGA setups were used and the experiments were performed in a Netzsch 449F3 and also in a custom-built larger instrument. The experiments in the Netzsch 449F3 will be referred to as regular TGA and the experiments in the custom-built instrument as Macro TGA. The main difference between the two is that in the Macro TGA reducing gas such as H_2 can be used while this is not the case for the regular TGA. The Macro TGA is also larger and the sample size in those experiments were roughly 1.5 g compared to 10-15 mg in the regular TGA. Both methods had the sample in a fixed bed set-up.

2.3.1 Regular TGA

At the beginning of a run, the sample was heated up to 850 °C from room temperature. One cycle consisted of 30 minutes at 850 °C and one hour at 900 °C and each sample was put through 5 cycles. The rate of the temperature change between the two phases was 20 °per minute and the rate was kept constant during the experiment, bringing a full cycle to 1 hour and 35 minutes. During the phase with 900 °C a gas flow of 90 ml per minute of either N_2 or CO_2 was used to create an inert atmosphere. CO_2 was only used in one early experiment and was later replaced with N_2. A mix of 20 vol% oxygen and 80 vol% N_2 at a flow rate of 90 mL per minute were used for the remaining phases to create a reducing atmosphere.
Beyond this original TGA experiment design, further tests were done with different temperatures to evaluate the performance in a potential CLC process. Other than changing the temperatures no changes were done. The other temperature setups tested were 850-850, 900-900, 850-950 and 850-1000 where the first number is the temperature during the oxidizing phase and the other is the temperature during the inert phase.

2.3.2 Macro TGA

The schematics of the custom-built macro TGA is shown in Figure 2.2. The instrument consisted of two furnaces, one to evenly preheat the gas and one where the reaction between the gas and oxygen carrier took place. Inside the ovens was a quartz tube with an inner diameter of 8 cm. The sample holder was 4x4 cm in length and width and the height was 0.3 cm and made of quartz. The sample was evenly distributed onto the sample holder in order to minimize the impact of mass transport resistance. The compartment with the ovens was fixed on a rail and could be moved up and down with a motor. That way the sample could quickly be moved inside the preheated oven.

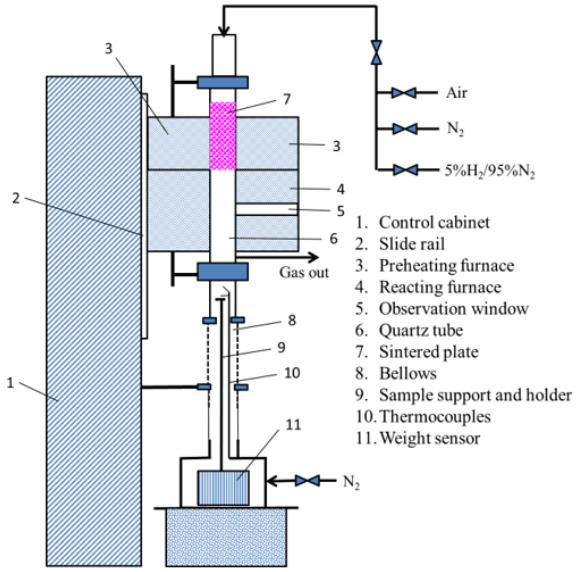

Figure 2.2: A schematic overview of the macro TGA instrument [44].

The temperature was kept at 850 °C during one full cycle and an experiment consisted of five cycles in general but occasionally of six cycles. Three different gas flows were used to create different atmospheres. N_2-gas was used to create an inert atmosphere, 21% O_2 mixed with N_2 to create an oxidizing atmosphere and 5% H_2 mixed with N_2 to create a reducing atmosphere. The gas flow, which was constant for all three phases, was 1 L/min and the heating rate was 20 °C. The oxidizing phase lasted 3 minutes and the reducing phase lasted 10 minutes. Before switching between a reducing and oxidizing phases there was a two-minute long inert period.

2.4 Melting characteristics

The analysis of the oxygen carriers melting characteristics was done with a novel optical camera-image system which is illustrated in Figure 2.3. A gas source is connected to a chamber with a heating zone. The chamber is monitored with a camera that captures footage of the sample during the melting and the temperature

is monitored with a thermometer. A mold which had seven tetrahedral holes in it had been designed and produced out of corundum. The tetrahedrons had a height of 20 mm high and all sides of the base were 7 mm.

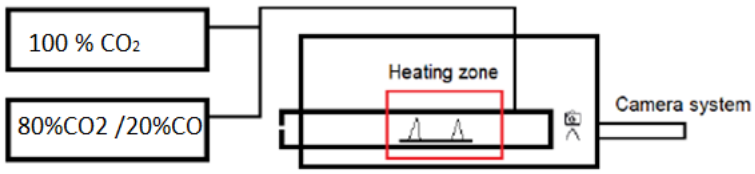

Figure 2.3: A schematic overview of the experimental setup for the measurement of the melting characteristics.

The sample was placed in the mold to form the sample into a tetrahedral shape. After the tetrahedral was extracted out of the mold it was then put in the heating zone where it was illuminated to clearly see the contours of the tetrahedral during the melting experiment. Melting experiments were done with both a reducing and an oxidizing environment and the experiment progressed at 18 °C per minute until it reached 1500 °C where it was aborted. The camera system worked at 20 fps meaning it took 20 pictures per second. The pictures were then manually examined to identify at which temperatures the different phases occurred.

Five different melting stages were defined and are illustrated in Figure 2.4. The first stage is the prototype temperature (PT) which is at the first sign of melting, usually when the tip loses its sharp edge. The deformation temperature (DT) is defined as when the edge or tip bends or becomes round. Softening temperature (ST) is when the tip bends to an extent that it is touching the tray or it becomes spherical. When the height of the cone is half of the length of the base, or the shape is approximately a hemispherical it has reached the hemispherical temperature (HT). When the cone is fully melted and the height is below 1.5 mm the flow temperature (FT) is reached. For an oxygen carrier, it is mainly the PT that is relevant. At this temperature, the outer layer of the particle has started to smelt and it becomes sticky. When the particles become sticky there is a risk that they get stuck to other particles, forming agglomerates which could impede the fluidization.

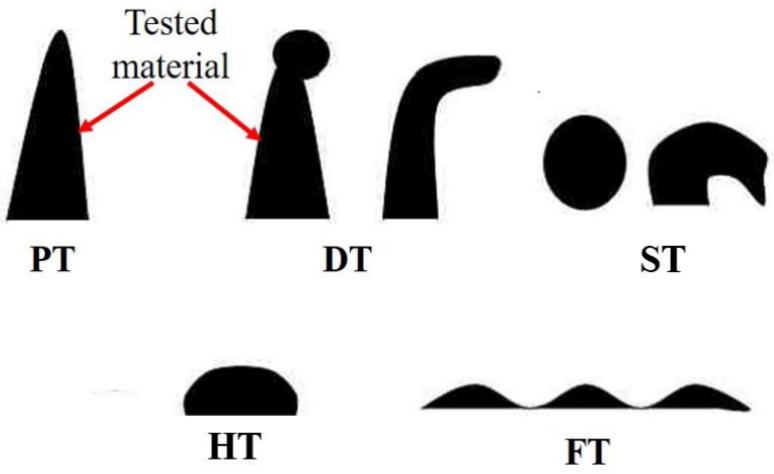

Figure 2.4: The five different melting stages of the sample tetrahedral is illustrated [45].

Fluidization related issues are normally reported after being tested in a fluidized setting such as a single fluidized bed reactor or in a CLC process. This experimental procedure seeks to create an easy method to test agglomeration issues before testing it further and also creating a standardized test, making it easier to compare oxygen carriers to each other.

2.5 Data evaluation

This section briefly describes the methods used to evaluate the data from the regular and macro TGA experiments. As well as the kinetic model that was used.

2.5.1 Regular TGA

The weight change of a sample was considered to be the average from the five TGA cycles each sample experienced. The weight change in one cycle was calculated as the difference in weight between the value where the oxidizing phase changed to the inert phase and the lowest value measured during the inert phase in the cycle. The sensitivity of the instrument was high which lead to that the data could fluctuate at seemingly random times. To minimize this uncertainty precautions were taken. Instead of selecting the value at the start of the inert phase as the highest value, 21 values were selected around this point and the 3:rd highest of these were selected as the maximum value. A similar approach was taken towards finding the lowest value of the phase. One inert phase consisted of 1200 data points and the 20:th lowest value were chosen as the lowest. These two procedures were done to minimize the effect of outliers in the data.

2.5.2 Macro TGA

Due to the scale used in the experiment being a lot less precise than the one in the Regular TGA the data was as a consequence less meticulous. The weight change was therefore simply considered the difference between the highest and lowest values for one cycle.

2.5.3 Kinetic model

The amount of oxygen released from an oxygen carrier is an important parameter but another important parameter is the rate of the release. To investigate this a simple kinetic model was produced and implemented on the regular TGA data. The ratio of the weight change during the initial 10 minutes and the weight change during the whole phase. Instead of using the value at 10 minutes into the experiment directly, five data points before and after were also included and an average was calculated for these 11 data points. The total weight loss during the same phase was divided by this value to get the ratio. A ratio of 1 therefore means that all oxygen released during the cycle were released during the first 10 minutes.

3
Results

3.1 Crushing test

The results from the crushing tests are presented in Table 3.1 below. Without any added kaolin the LY ore had a crushing strength of 3.1N and the FJ ore oxygen carrier had a crushing strength of 5.7N. The FJ particles with the lower sintering temperature had a strength of 3.9N. The crushing strength was increased with the addition of kaolin for both of the ore types tested. LY saw the biggest increase where 5 wt% increased it to 53.5N but the addition of even more kaolin did not improve it further with 52.8 and 48.6N for 10 and 15 wt% kaolin respectively. FJ with 5 wt% added nearly doubled in strength and almost saw a triple increase with 10 wt% added.

Table 3.1: The force required to crush one particle of each oxygen carrier.

Oxygen carrier	Crushing strength [N]
FJ-Mn0-950	3.9
FJ-Mn0-1100	5.7
FJ-Mn5-1100	9.3
FJ-Mn10-1100	16.3
LY-Mn0-1100	3.1
LY-Mn5-1100	53.5
LY-Mn10-1100	52.8
LY-Mn15-1100	48.6

3.2 Regular TGA

Several regular TGA tests were done to examine the effect on the CLOU properties when adding kaolin to the manganese ores and also the effect on the same properties by impregnating the ore with copper and calcium.

3.2.1 Addition of kaolin

Presented below in Figure 3.1 and Figure 3.2 are the TGA results from the LY ore mixed with kaolin. In a N_2 atmosphere the sample without any kaolin had an

oxygen release capacity of 0.397 wt%. The capacity was decreased with the addition of more kaolin where LY-Mn5-1100 had a capacity of 0.168, LY-Mn10-1100 0.108 and LY-Mn15-1100 had the lowest at 0.070 wt%.

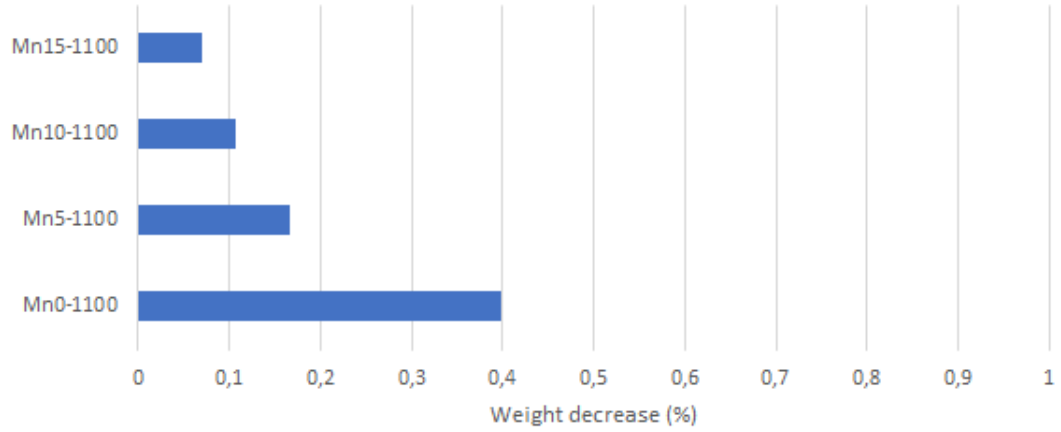

Figure 3.1: The average weight decrease for LY oxygen carriers with different kaolin content in a N_2 environment.

The same ore with added kaolin was tested in an additional test with CO_2 as the inert gas during the inert phases. The trend observed was similar to the previous one where the ore without any kaolin had the highest CLOU properties by a large margin as can be seen in 3.2. With the addition of kaolin, the CLOU properties of the oxygen carriers saw a clear decrease. A difference from the previous tests in N_2 however was that the difference in oxygen release capacities between LY-Mn5-1100 and LY-Mn10-1100 was lower. LY-Mn5-1100 and LY-Mn10-1100 had an oxygen release capacity of 0.158 and 0.154 wt% respectively and LY-Mn15-1100 had 0.098. The weight decrease of LY-Mn0-1100 was 0.539 wt%. In general, the oxygen release was higher in CO_2 atmosphere than N_2.

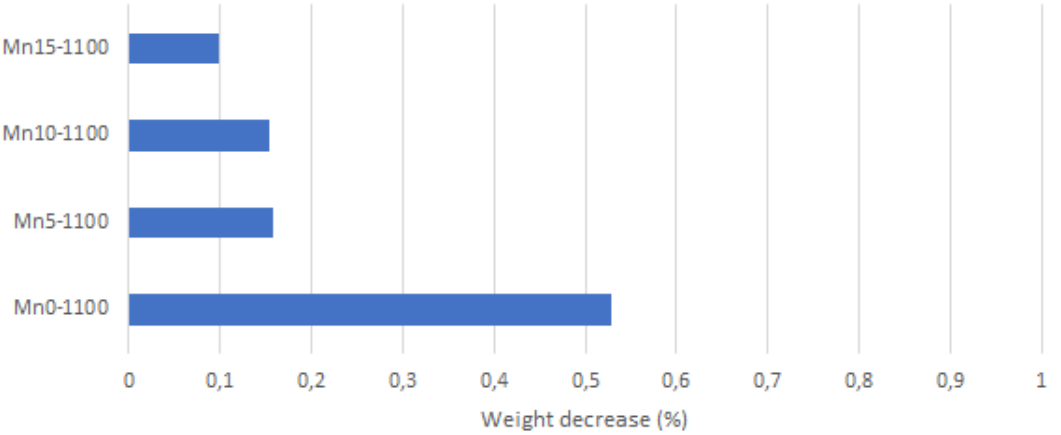

Figure 3.2: The average weight decrease for LY oxygen carriers with different kaolin content in a CO_2 environment.

For the FJ ore, the two samples with no added kaolin showed the biggest CLOU properties. The oxygen carrier with a sintering temperature of 950 °C, FJ-Mn0-950, had a weight loss of 1.03 % while FJ-Mn0-1100 showed an average weight loss of 0.868 wt%. The weight loss for FJ-Mn5-1100 was 0.60 and FJ-Mn10-1100 experienced the lowest weight change in this series at 0.115 % weight change. In N_2, the CLOU properties for FJ was higher than LY. One exception was the Mn10-1100 however with a different inert gas.

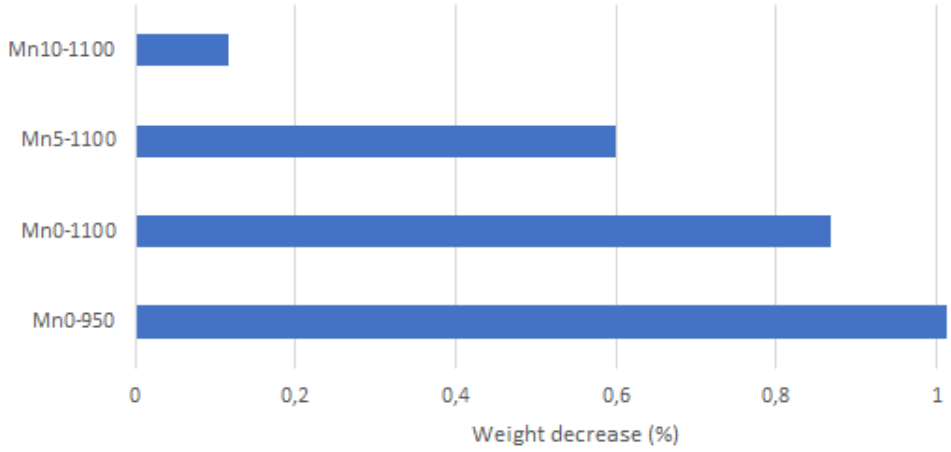

Figure 3.3: The average weight decrease for FJ oxygen carriers with different kaolin content in N_2 environment.

3.2.2 Impregnation

Impregnation trials were done with both calcium and copper and the TGA results are presented below. Mn5-1100 was selected for impregnation for both ores.

3.2.2.1 Copper

LY-Mn5-1100 that was tested previously had an oxygen release capacity of 0.174 wt% in the TGA experiment with N_2. After the impregnation with copper, the CLOU properties of the oxygen carriers increased. The oxygen release capacity of LY-Mn5-1100-Cu0.5 was 0.269, 0.235 for LY-Mn5-1100-Cu2 and for Mn5-1100-Cu5 it was 0.498 wt%. It is notable that the sample with 2 wt% added copper showed lower CLOU properties than the sample with 0.5 wt% copper.

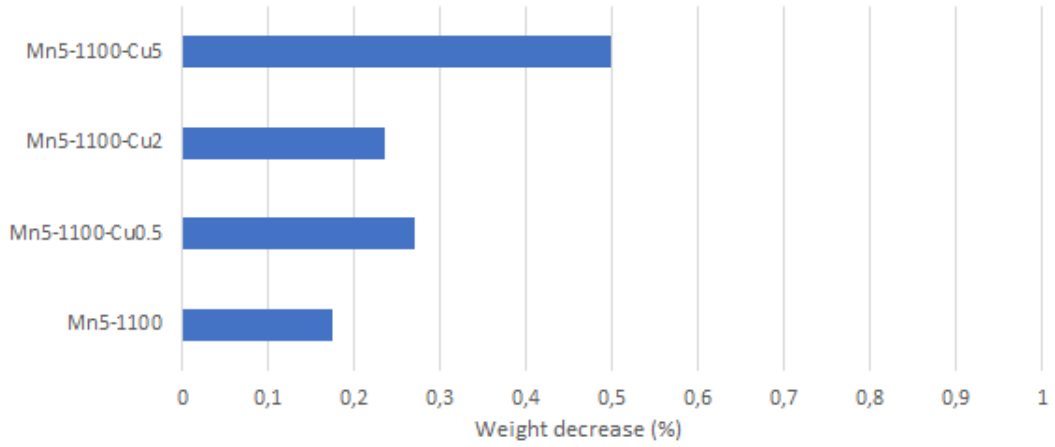

Figure 3.4: The average weight decrease for LY-Mn5 oxygen carriers impregnated with different copper content in a nitrogen environment.

The difference between the FJ-Mn5-1100-blank and the previously tested FJ-Mn5-1100 was 0.06 wt%. The weight change for the sample tested earlier was 0.60 % and the blank sample tested together with the impregnated samples was 0.54 %. All samples impregnated with copper saw an increase in weight change and the samples with more copper saw a bigger increase. FJ-Mn5-1100-Cu0.5, FJ-Mn5-1100-Cu2 and FJ-Mn5-1100-Cu5 had an oxygen release capacity of 0.656, 0.739 and 0.968 wt% respectively.

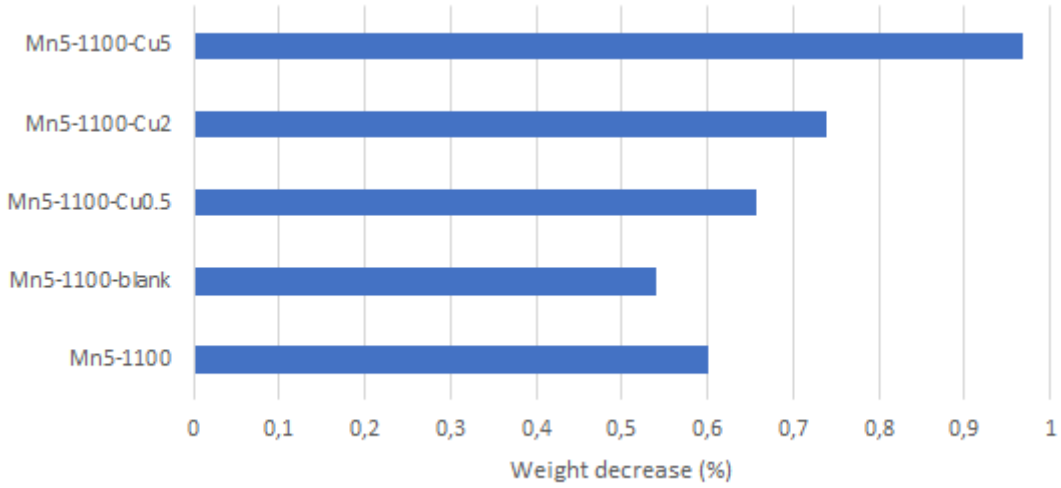

Figure 3.5: The average weight decrease for FJ-Mn5 oxygen carriers impregnated with different copper content in a nitrogen environment. Also included is the blank sample and the previously tested Mn5-1100.

3.2.2.2 Calcium

The results from the regular TGA for the calcium impregnated FJ-Mn5 oxygen carrier, shown in Figure 3.6, indicated no improvement in oxygen release capacity.

Because of the positive results with the copper impregnation no further trials were made with calcium impregnation.

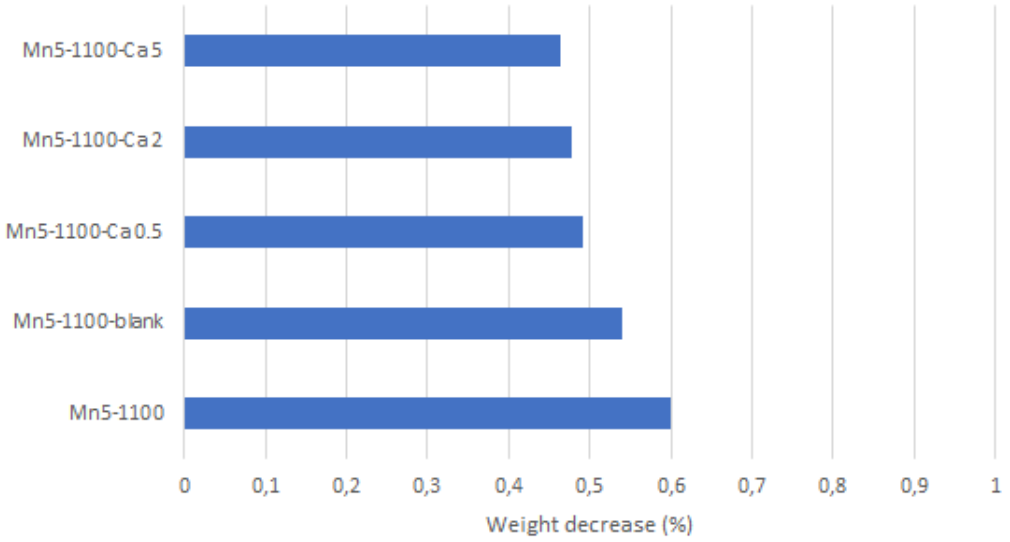

Figure 3.6: The average weight decrease for FJ-Mn5 oxygen carriers impregnated with different calcium content in a nitrogen environment.

3.2.3 Post redox tests

To investigate the impact of redox cycles on the oxygen carriers, additional regular TGA tests were performed after the oxygen carriers had been tested in the macro TGA. A few oxygen carriers of each ore were selected and compared to the previous results for the same oxygen carrier. The results are shown in Figure 3.7 and Figure 3.8 below. All samples of the LY ore tested both before and after the macro TGA showed an increase in CLOU properties. The LY-Mn5-1100-Cu5 experienced a slight increase while the other experienced an increase of a factor of 1.87 or more.

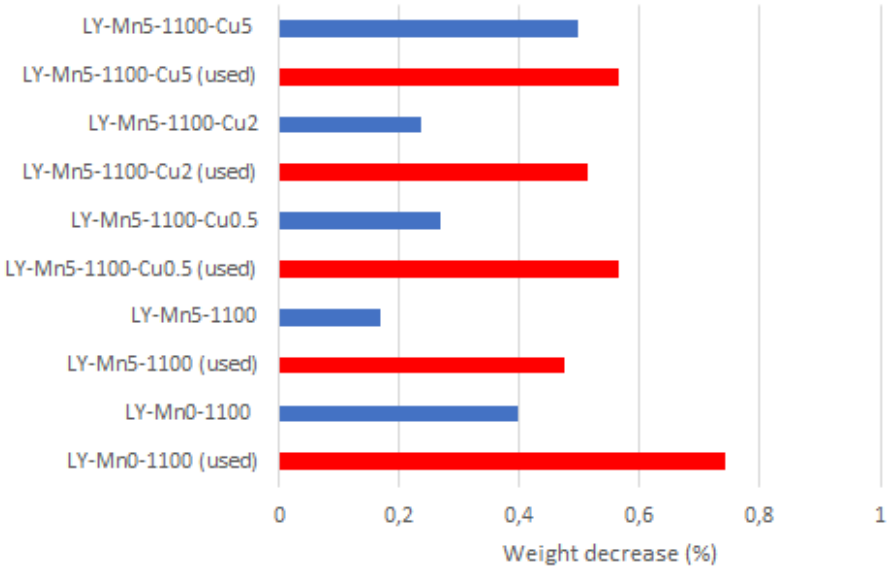

Figure 3.7: The weight decrease from different LY oxygen carriers both before and after the macro TGA. The samples tested in both regular and macro TGA are marked in red color and samples not tested in the macro TGA are in blue.

Contrary to the LY samples the oxygen carriers made from the FJ ore all saw a decrease in CLOU properties after the macro TGA test. The oxygen release capacity of FJ-Mn0-1100 decreased to roughly one third. The three impregnated samples tested, also exhibited a decrease in oxygen release capacity after the macro TGA although not as large as FJ-Mn0-1100. Of the impregnated samples, FJ-Mn5-1100-Cu5 had the biggest decrease in oxygen release capacity followed by FJ-Mn5-1100-Cu2.

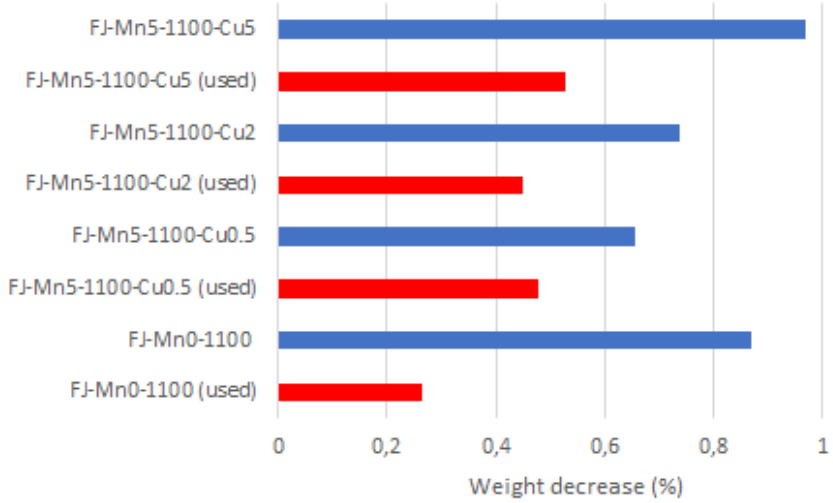

Figure 3.8: The weight decrease from different FJ oxygen carriers both before and after the macro TGA. The samples tested in both regular and macro TGA are marked in red color and samples not tested in the macro TGA are in blue.

3.2.4 Temperature investigation

Additional measurements in the regular TGA were performed with different temperature for the cycles. In the original TGA cycle design the oxidizing phase occurred at 850 °C and the inert phase at 900 °C. Below in Figure 3.9 are the average oxygen release capacity from the TGA experiment and the tested cycle designs were 850-850, 850-950 and 900-900 cycles which were compared to their counterpart tested in an 850-900 cycle. All samples tested were manufactured from the FJ ore. Both TGA cycles with the same temperature in both phases, 850-850 and 900-900, showed performance below the 850-900 cycle. The Mn5-1100-Cu2 increased its oxygen release capacity with 0.257 wt% in the 850-950 program.

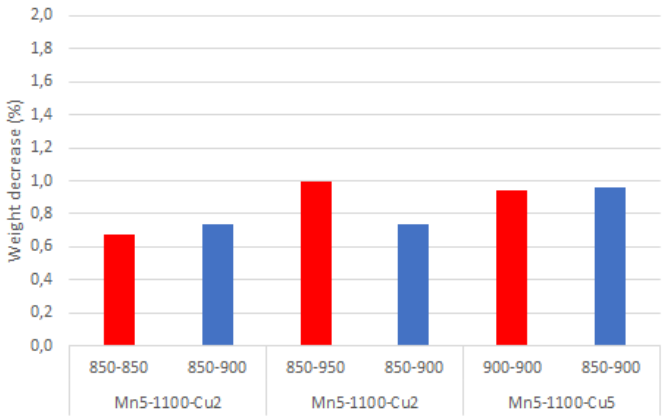

Figure 3.9: Weight decrease for different FJ-Mn5 oxygen carriers ran at different temperature setups. 850-850, 850-950 and 900-900 were compared to the original 850-900 setup.

Both 850-950 and 850-1000 cycles were tested and out-performed the 850-900 cycle for every sample compared. The biggest difference was seen for the FJ-Mn0-1100 sample which had an oxygen release capacity of more than twice as large at 850-1000 than at 850-900. The increase for Mn5-1100 was 0.119 but the increase for the impregnated oxygen carriers was larger. The oxygen release capacity for Mn5-1100-Cu0.5 increased with 0.454 and 0.201 for Mn5-1100-Cu2.

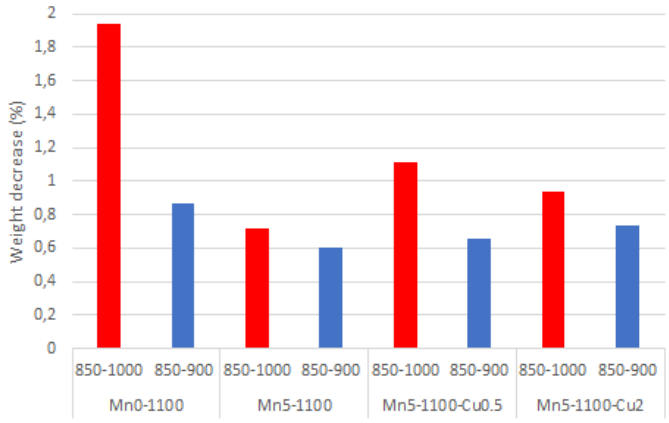

Figure 3.10: Weight decrease for different FJ-Mn5 oxygen carriers ran at different temperature setups. 850-1000 were compared to the original 850-900 setup.

3.2.5 Kinetic model

The average ratio for all five cycles was calculated for several oxygen carriers to see if any change could be observed. A general observation was that the majority of the oxygen was released during the first 10 minutes. The average ratio for all oxygen carriers was 0.811, meaning that 81 % of the total oxygen released was released during the first 10 minutes. The copper impregnated oxygen carriers had an average ratio of 0.805 while the ratio of those without impregnation was 0.770. The used samples as in those tested after the macro TGA had a higher average ratio of 0.875.

The average ratio for each of the five cycles for three oxygen carriers can be seen in Figure 3.11. The oxygen carriers included FJ-Mn5-Cu-0.5, FJ-Mn5-Cu-2 and FJ-Mn5-Cu-5. The oxygen carriers demonstrated the quickest oxygen release during the first cycle with a ratio of 0.898. The following cycles had lower ratios with the fifth being the lowest at 0.694.

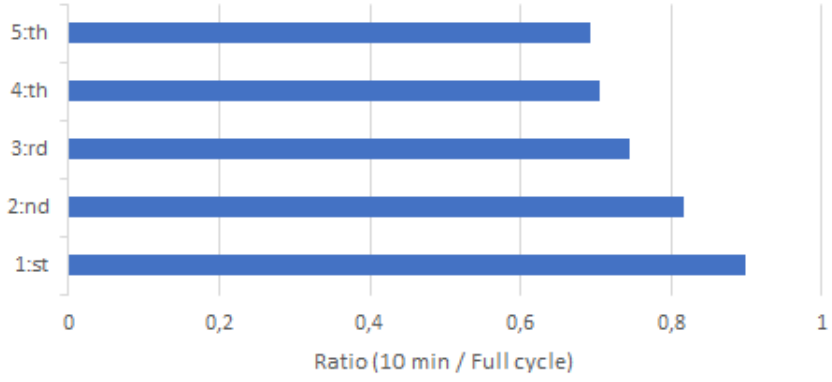

Figure 3.11: The average ratios for the combined three impregnated FJ-Mn5-1100 samples for each of the five regular TGA cycles.

Oxygen carriers made out of LY ore also showed the same behavior. The average

ratio of the first cycle for the samples was the highest at 0.979. The second had a ratio of 0.880 and the third 0.791. The third, fourth and fifth all had quite similar ratios.

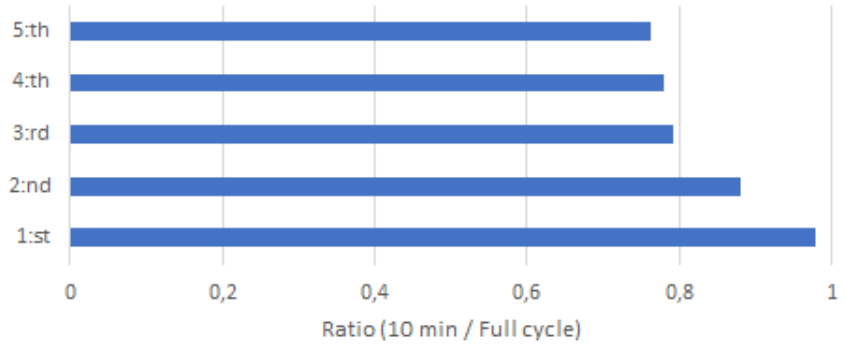

Figure 3.12: The average ratios for the combined three impregnated LY-Mn5-1100 samples for each of the five regular TGA cycles.

This tendency between the cycles was not as obvious in other sample series. The data in Figure 3.13 below is the average for the different cycles from FJ-Mn0-950, FJ-Mn0-1100, FJ-Mn5-1100 and FJ-Mn10-1100 combined. The highest ratio was again during the first cycles but the difference between the highest and the lowest ratios was 0.074 indicating a low change from cycle to cycle.

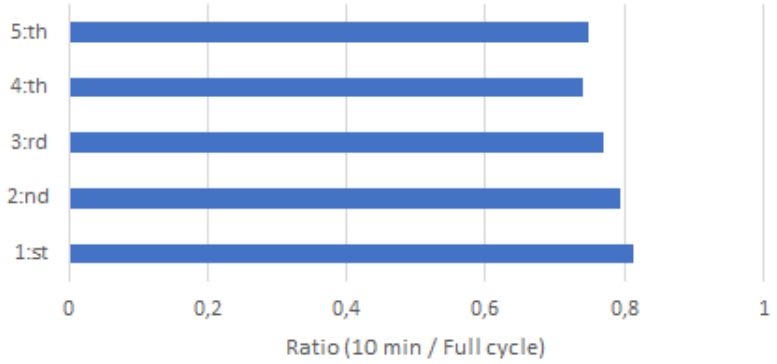

Figure 3.13: The average ratios for the combined four FJ-Mn-1100 samples for each of the five regular TGA cycles.

The same data but for the LY ore oxygen carriers showed that the first cycles had a quicker release but the difference between the following four were low. The difference between the ratio of the first and the second cycle was 0.118 but after that change the change between cycles was small.

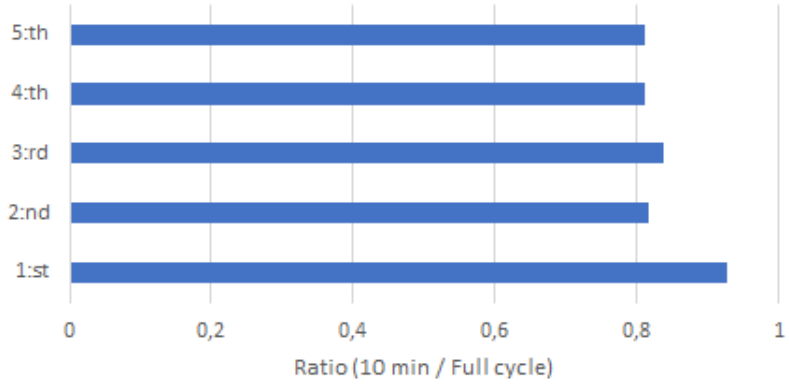

Figure 3.14: The average ratios for the combined four LY-Mn-1100 samples for each of the five regular TGA cycles.

3.3 Macro TGA

In order to evaluate the capability of fuel conversion of the oxygen carriers, macro TGA trials were performed. The weight loss in the macro TGA was much higher compared to the regular TGA, due to the phase with the reducing atmosphere which was not present during the regular TGA tests.

3.3.1 Addition of kaolin

The weight loss was highest for LY-Mn0-1100 and it decreased with an increase in kaolin content. The highest weight decrease in the series was 5.217 % and the lowest was 2.098 %.

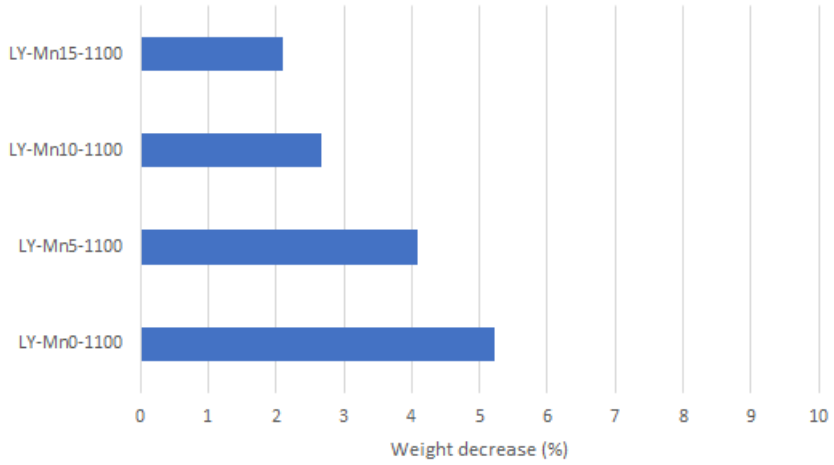

Figure 3.15: The average weight decrease in % for the LY oxygen carriers from the macro TGA experiments.

The samples with the FJ ore had a higher weight change during the cycles than those with the LY. As for LY the addition of kaolin decreased the weight change.

FJ-Mn5-1100 experienced a weight decrease of 8.209 %, FJ-Mn5-1100 6.162 % and the weight decrease for FJ-Mn10-1100 5.254 %.

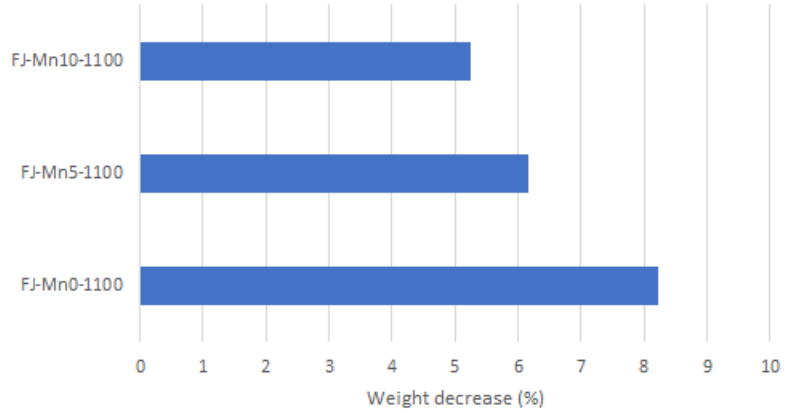

Figure 3.16: The average weight decrease in % for the FJ oxygen carriers from the macro TGA cycles experiments.

3.3.2 Impregnation

The impregnation with copper of the LY-Mn5-1100 oxygen carriers did not show a big impact. With the 0.5 wt% recipe the performance slightly decreased and 2 and 5 wt% copper only saw a very slight increase in weight decrease during the cycles. The weight loss for LY-Mn5-1100 was 4.084 and the maximum weight loss was 4.929 %, an increase of 0.845 percentage.

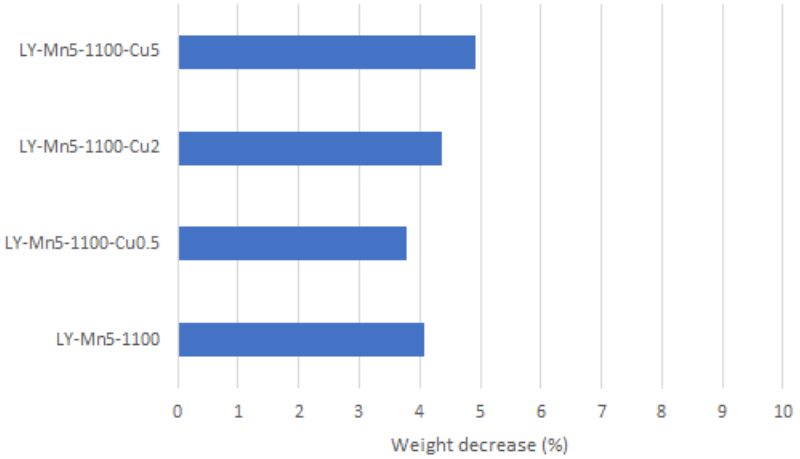

Figure 3.17: The average weight decrease in % for the impregnated LY samples from the five macro TGA cycles.

The FJ-Mn5-1100 oxygen carrier responded better to the copper impregnation. The FJ oxygen carrier, which also performed better before the impregnation, was enhanced more by the impregnation than the LY counterpart. The maximum percent-

age improvement for the FJ was 2.915, more than three times the improvement of LY.

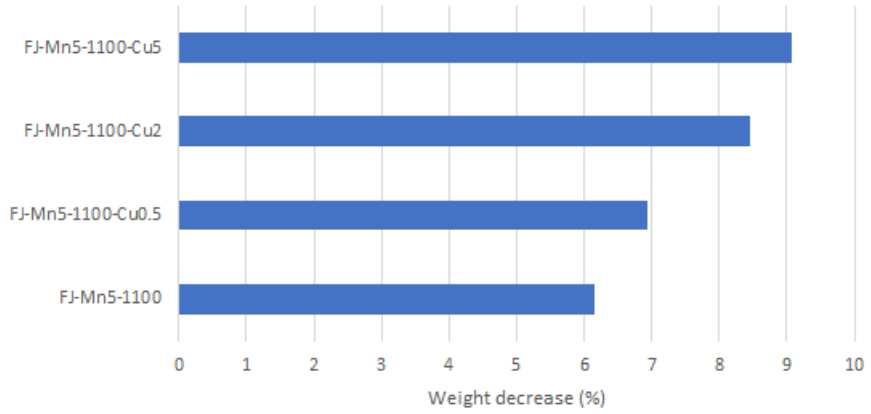

Figure 3.18: The average weight decrease in % for the impregnated FJ samples from the five macro TGA cycles.

3.4 Melting characteristics

The addition of kaolin increased the prototype temperature for every sample in both atmospheres and the more kaolin added, the more the prototype temperature increased. For the FJ ore the difference between Mn0-1100 and Mn10-1100 was 88 °C while for the LY ore, the difference between Mn0-1100 and Mn15-1100 was only 30 °C. In the case of LY, the Mn5-1100 rendered the highest temperature in soften, hemispherical and flowing temperature compared to oxygen carriers with more kaolin. The oxygen carrier with a higher sintering temperature had a higher prototype and deformation temperature but it had a lower soften, hemispherical and flowing temperature. This was true for both the inert and the reducing atmosphere.

Table 3.2: Temperatures for the different melting stages of the sample tetrahedral in an inert (CO_2) atmosphere.

Oxygen carrier	Prototype	Deformation	Soften	Hemispherical	Flowing
FJ-Mn0-950	1059°C	1342°C	1455°C	1470°C	1488°C
FJ-Mn0-1100	1082°C	1363°C	1425°C	1434°C	1455°C
FJ-Mn5-1100	1106°C	1405°C	1450°C	1468°C	1494°C
FJ-Mn10-1100	1170°C	1416°C	1457°C	1473°C	>1500°C
LY-Mn0-1100	1109°C	1208°C	1249°C	1261°C	1311°C
LY-Mn5-1100	1121°C	1290°C	1339°C	1355°C	1417°C
LY-Mn10-1100	1128°C	1268°C	1327°C	1340°C	1374°C
LY-Mn15-1100	1139°C	1243°C	1288°C	1304°C	1315°C

All melting stages for every kind of oxygen carrier tested occurred at a lower tem-

perature in a reducing atmosphere than it did with an inert atmosphere.

Table 3.3: Temperatures for the different melting stages of the sample tetrahedral in a reducing (CO/CO_2) atmosphere.

Oxygen carrier	Prototype	Deformation	Soften	Hemispherical	Flowing
FJ-Mn0-950	1010°C	1318°C	1420°C	1449°C	1463°C
FJ-Mn0-1100	1045°C	1348°C	1414°C	1431°C	1448°C
FJ-Mn5-1100	1060°C	1301°C	1392°C	1394°C	1440°C
FJ-Mn10-1100	1122°C	1348°C	1371°C	1380°C	1391°C
LY-Mn0-1100	1059°C	1207°C	1224°C	1226°C	1229°C
LY-Mn5-1100	1082°C	1227°C	1237°C	1241°C	1246°C
LY-Mn10-1100	1098°C	1229°C	1236°C	1242°C	1246°C
LY-Mn15-1100	1123°C	1231°C	1238°C	1240°C	1246°C

Three impregnated samples of the FJ ore were tested and are presented in Figure 3.4. The difference in prototype temperature between FJ-Mn5-1100 and the samples impregnated with 0.5 and 2 wt% was small, only 4 and 9 °C. The difference between FJ-Mn5-1100 and FJ-Mn5-1100-Cu5 was larger, which was 50 °.

Table 3.4: Temperatures for the different melting stages of the sample tetrahedral in an inert (CO_2) atmosphere.

Oxygen carrier	Prototype	Deformation	Soften	Hemispherical	Flowing
FJ-Mn5-1100-Cu0.5	1102°C	1400°C	1445°C	1461°C	1489°C
FJ-Mn5-1100-Cu2	1095°C	1393°C	1440°C	1455°C	1481°C
FJ-Mn5-1100-Cu5	1056°C	1347°C	1395°C	1408°C	1435°C

4
Discussion

The modifications done to the manganese ores resulted in positive improvements in their properties with rather simple methods. The crushing tests suggested that the LY ore was weaker from the beginning but saw a bigger improvement than the FJ by adding kaolin. Compared to other studies the measured values are quite high but the reason for this could be tied to the specific instrument or the operator performing the experiments. Since every equipment is different it is possible that if the oxygen carriers were tested on other instruments the result would be lower. However, the important factor is that the improvement was large, rather than how large it was. The crushing strength of FJ-Mn0-1100 was increased to almost three times as much and for LY-Mn0-1100 it was increased more than 15 times. The kaolin additive did however lower the reactivity of the ore.

The oxygen carriers impregnated with copper after the addition of kaolin all saw an increase in CLOU properties and the increase was bigger with more copper except for a few exceptions. There were however differences between FJ and LY in terms of performance. Without any modifications the FJ, ore had better CLOU properties as well as larger fuel conversion during the redox cycles. The impregnation seemed to affect the FJ slightly more than the LY ore in the regular TGA. The difference was bigger in the macro TGA were FJ performed better which should be an indication of fuel conversion ability. To test if the impregnation effect wore off with time, additional TGA tests were done after the redox cycles in the macro TGA. The impregnated FJ-Mn5-1100 oxygen carrier demonstrated this behavior where every sample tested additionally had a lower oxygen release capacity. While all of the three impregnated FJ-Mn5-1100 samples tested had decreased CLOU properties but FJ-Mn0-1100, a sample without any impregnation, showed the same behavior. This point towards a reaction in the oxygen carrier during the redox cycles rather than that the impregnation wearing off. However the same was not true for the LY samples tested, where every sample improved their CLOU properties after the redox cycles in the macro TGA. The sample impregnated with 5 wt% copper saw a lower change than samples impregnated with less copper or no copper at all also indicating that this change is not tied to the impregnation.

The reason for the differences between the two ores is not known but the fact that their composition is different might be the reason. The LY ore has a higher content of manganese while the FJ had a much higher potassium content and slightly higher iron content. Further analysis of the ores could give clues to why this difference occurred. Example of such analysis is SEM, EDX or XRD that could give more

information on the interaction between the ore and kaolin and the effect of the impregnation. Since the ores sometimes responded differently to the same treatment, it could motivate some criticism in the methodology. For example the FJ ore was not tested with 15 wt% kaolin and no melting characteristic trials were performed with the impregnated LY oxygen carriers. The melting characteristics analysis was not performed on the LY-Mn5-1100-Cu oxygen carriers because the decrease was not very large for the FJ oxygen carriers. Because the response differed between the two ores there is a possibility that the LY ore would have rendered a different result.

In a CLC process, the oxygen carrier is cycled between the air reactor and fuel reactor, releasing and taking up oxygen. Not only the amount of oxygen that the oxygen carrier can release is important but at what rate it happens. A high rate would make it possible for fast cycling between the reactors, lowering the amount of oxygen carrier needed. The kinetic model was used in an attempt to show any connections between the rate and the different treatments performed on the oxygen carriers. The model found that in general 80 % of the oxygen release happened the first 10 minutes. The model also showed signs of some differences between impregnated oxygen carriers and oxygen carriers without. For the impregnated samples the rate was higher during the initial cycles and the rate was declining but seemed to stabilize. This phenomenon might only occur during the very first cycles, but if that was the case could not be concluded by the trials that were done. Other than these observations no further conclusions could be drawn using the model. 10 minutes could be considered too long time in a CLC process and it is possible that a model using a shorter period, for example 2-3 minutes, would have been more suiting.

The temperatures used in the TGA tests could help determine an optimal setup for a CLC process where the air reactor would have the same temperature as the oxidizing phases and the temperature in the fuel reactor the same as for the inert phase. However, the melting characteristics tests showed that the sintering temperature is lower in a reducing atmosphere than an inert atmosphere. The temperature investigations done in this report show that a higher temperature leads to better CLOU properties with a larger oxygen release which should improve the efficiency of the reaction. However an increased temperature would be more energy demanding and further investigations on how much more energy it would require compared to the efficiency increase would be needed in order to determine the optimal temperatures. Increase the operation temperature would also increase the risk of agglomeration with fluidization issues as a consequence.

Further evaluating of the oxygen carriers should be done with fluidized bed tests or tests in a pilot CLC setups. Testing in an environment that is similar to the real use is needed to estimate the lifetime of the oxygen carriers. Also extended testing to ensure that the impregnation will last long enough for it to be meaningful to implement. The FJ-Mn5-1100-Cu2 should be a good candidate considering the good CLOU properties and reactivity while having seemingly good physical properties. Additional analyzing of the oxygen carriers could give a deeper understanding of

why the different ores have a different responses to the same treatment. An XRD analysis to see which phases are formed between the kaolin and the components in the different ores could help to answer that.

5
Conclusion

Several different types of oxygen carriers were manufactured and evaluated. The two natural manganese ores, FJ and LY, had different elemental compositions and showed different properties. The following can be concluded:

- Kaolin added to manganese ores increases the crushing strength and increases the sintering temperature.
- The addition of kaolin also decreases CLOU properties and fuel conversion abilities.
- Impregnating with copper which improves the CLOU properties and fuel conversion works together when using kaolin as additive.
- Impregnation with calcium did not show any signs of improving the oxygen carrier.

From the experiments done the FJ-Mn5-1100-Cu2 oxygen carrier was decided to be the most promising one due to its reactivity and physical properties. Suggesting the TGA results it has better reactivity than the FJ-Mn0-1100 oxygen carrier while being stronger. It was also found that CLOU properties increased with increased temperature but the total efficiency of this temperature remains to be investigated.

Bibliography

[1] IPCC. Climate Change 2014. Synthesis Report. Contribution of Working Groups I, II and III to the Fifth Assessment Report of the Intergovernmental Panel on Climate Change. 2014;.

[2] IPCC. Carbon Dioxide Capture and Storage. 2005;.

[3] Manancourt A, Gale J. A review of capacity estimates for the geological storage of carbon dioxide. Greenhouse Gas Control Technologies. 2005;Vol. 2:2051–2054.

[4] Kanniche M, Gros-Vonnivard R, Jaud P, Valle-Marcos J, Amann J, Bouallou C. Pre-combustion, post-combustion and oxy-combustion in thermal power plant for CO_2 capture. Applied Thermal Engineering. 2010;Vol. 30:53–62.

[5] Scholes C, Smith K, Kentish S, Stevens G. CO_2 capture from pre-combustion processes - Strategies for membrane gas separation. International Journal of Greenhouse Gas Control. 2010;Vol. 4:739–755.

[6] Merkel T, Lin H, Wei X, Baker R. Power plant post-combustion carbon dioxide capture: An opportunity for membranes. Journal of Membrane Science. 2010;Vol. 359:126–139.

[7] Buhre B, Elliott L, Sheng C, Gupta R, Wall T. Oxy-fuel combustion technology for coal-fired power generation. Progress in Energy and Combustion Science. 2005;Vol. 31:283–307.

[8] Lyngfelt A, Leckner B, Mattison T. A fluidized-bed combustion process with inherent CO_2 separation; application of chemical-looping combustion. Chemical Engineering Science. 2001;Vol. 56:3101–3113.

[9] Rydén M, Leion H, Mattisson T, Lyngfelt A. Combined oxides as oxygen-carrier material for chemical-looping with oxygen uncoupling. Applied Energy. 2014;Vol. 113:1924–1932.

[10] Pérez-Vega R, Abad A, García-Labiano F, Gayán P, de Diego L, Izquierdo M, et al. Chemical Looping Combustion of gaseous and solid fuels with manganese-iron mixed oxide as oxygen carrier. Energy Conversion and Management. 2018;Vol. 159:221–231.

[11] Mendiara T, García-Labiano P, P G, Abad A, de Diego L, J A. Evaluation of the use of different coals in Chemical Looping Combustion using a bauxite waste as oxygen carrier. Fuel. 2013;Vol.106:814–826.

[12] Marx K, Bertsch O, Pröll T, Hofbuaer H. Next scale chemical looping combustion: Process integration and part load investigations for a 10MW demonstration unit. Energy Procedia. 2013;Vol.37.

[13] Lyngfelt A, Leckner B. A 1000 MWth boiler for chemical-looping combustion of solid fuels – Discussion of design and costs. Applied Energy. 2015;Vol.157:475–487.

[14] Wang P, Leion H, Yang H. Oxygen-Carrier-Aided Combustion in a Bench-Scale Fluidized Bed. Energy & Fuels. 2017;Vol. 31.

[15] M R, Hanning M, A C, Lind F. Oxygen Carrier Aided Combustion (OCAC) of Wood Chips in a Semi-Commercial Circulating Fluidized Bed Boiler Using Manganese Ore as Bed Material. Applied Sciences. 2016;Vol. 6:347–366.

[16] Tang M, Xu L, Fan M. Progress in oxygen carrier development of methane-based chemical-looping reforming: A review. Applied Energy. 2015;Vol. 151:143–156.

[17] Adanez J, Abad A, Garcia-Labiano F, Gayan P, de Diego F. Progress in Chemical-Looping Combustion and Reforming technologies. Progress in Energy and Combustion Science. 2012;.

[18] Adánez J, Dueso C, de Diego L, García-Labiano F, Gayán P, Abad A. Methane Combustion in a 500 W_{th} Chemical-Looping Combustion System Using an Impregnated Ni-Based Oxygen Carrier. Energy & Fuels. 2009;Vol. 23:130–142.

[19] C L, Abad A, Mattisson T, Lyngfelt A. 160 h of chemical-looping combustion in a 10 kW reactor system with a NiO-based oxygen carrier. International Journal of Greenhouse Gas Control. 2008;Vol. 2:520–530.

[20] Linderholm C, Mattisson T, Lyngfelt A. Long-term integrity testing of spray-dried particles in a 10-kW chemical-looping combustor using natural gas as fuel. Fuel. 2009;Vol. 88:2083–2096.

[21] Mattisson T, Jerndal E, Linderholm C, Lyngfelt A. Reactivity of a spray-dried $NiO/NiAl_2O_4$ oxygen carrier for chemical-looping combustion. Chemical Engineering Science. 2011;p. 4636–4644.

[22] Tian H, Chaudhari K, Simonyi T, Poston J, Liu T, Sanders T, et al. Chemical-looping Combustion of Coal-derived Synthesis Gas Over Copper Oxide Oxygen Carriers. Energy & Fuels. 2008;Vol. 22:3744–3755.

[23] Siriwardane R, Tian H, Richards G, Simonyi T, Poston J. Chemical-Looping Combustion of Coal with Metal Oxide Oxygen Carriers. Energy & Fuels. 2009;Vol. 23:3885–3892.

[24] Cao Y, Casenas B, Pan W. Investigation of Chemical Looping Combustion by Solid Fuels. 2. Redox Reaction Kinetics and Product Characterization with Coal, Biomass, and Solid Waste as Solid Fuels and CuO as an Oxygen Carrier. Energy & Fuels. 2006;Vol. 20:1845–1854.

[25] Cho P, Mattisson T, Lyngfelt A. Comparison of iron-, nickel-, copper- and manganese-based oxygen carriers for chemical-looping combustion. Fuel. 2004;Vol. 83.

[26] Mattisson T, Järdnäs A, Lyngfelt A. Reactivity of Some Metal Oxides Supported on Alumina with Alternating Methane and Oxygen - Application for Chemical-Looping Combustion. Energy & Fuels. 2003;Vol. 17.

[27] Mattisson T, Lyngfelt A, Leion H. Chemical-looping with oxygen uncoupling for combustion of solid fuels. International Journal of Greenhouse Gas Control. 2009;Vol.3:11–19.

[28] Jerndal E, Leion H, Axelsson L, Ekvall T, Hedberg M, Johansson K, et al. Using Low-Cost Iron-Based Materials as Oxygen Carriers for Chemical Looping Combustion. Oil & Gas Science and Technology. 2011;Vol. 66:235–248.

[29] Roux S, Bensakhria A, Antonini G. Study and Improvement of the Regeneration of Metallic Oxides Used as Oxygen Carriers for a New Combustion Process. International Journal of Chemical Reactor Engineering. 2006;Vol. 4.

[30] Schmitz M, Linderholm C, Lyngfelt A. Chemical looping combustion of four different solid fuels using a manganese-silicon-titanium oxygen carrier. International Journal of Greenhouse Gas Control. 70;Vol. 70.

[31] Adánez-Rubio I, Abad A, Gayán P, de Diego L, Adánez J. CLOU process performance with a Cu-Mn oxygen carrier in the combustion of different types of coal with CO2 capture. Fuel. 2018;Vol. 212.

[32] Abián M, Abad A, Izquierdo M, Gayán P, de Diego L, García-Labiano F, et al. Titanium substituted manganese-ferrite as an oxygen carrier with permanent magnetic properties for chemical looping combustion of solid fuels. Fuel. 2017;Vol. 195.

[33] Velasco-Sarria F, Forero C, Adánez-Rubio I, Abad A, Adánez J. Assessment of low-cost oxygen carrier in South-western Colombia, and its use in the *in-situ* gasification chemical looping combustion technology. Fuel. 2018;Vol. 218.

[34] Leion H, Mattison T, Lyngfelt A. Use of Ores and Industrial Products As Oxygen Carriers in Chemical-Looping Combustion. Energy & Fuels. 2009;Vol.23:2307–2315.

[35] Moldenhauer P, A S, F GL, de Diego L F, M B, T M, et al. Chemical-Looping Combustion of Kerosene and Gaseous Fuels with a Natural and a Manufactured MnFe-Based Oxygen Carrier. Energy & Fuels. 2018;Vol.32:8803–8816.

[36] Sundqvist S, Arjmand M, Matisson T, Ryden M, Lyngfelt A. Screening of different manganese ores for chemical-looping combustion (CLC) and chemical-looping with oxygen uncoupling (CLOU). International Journal of Greenhouse Gas Control. 2015;Vol.43:179–188.

[37] Schmitz M, Linderholm C, Hallberg P, Sundqvist S, Lyngfelt A. Chemical-Looping Combustion of Solid Fuels Using Manganese Ores as Oxygen Carriers. Energy & Fuels. 2016;Vol.30:1204–1216.

[38] Linderholm C, Knutsson P, Schmitz M, Markström P, Lyngfelt A. Material balances of carbon, sulfur, nitrogen and ilmenite in a 100 kWCLC reactor system. International Journal of Greenhouse Gas Control. 2014;Vol.27:188–202.

[39] Linderholm C, Schmitz M, Biermann M, Hanning M, A L. Chemical-looping combustion of solid fuel in a 100 kW unit using sintered manganese ore as oxygen carrier. International Journal of Greenhouse Gas Control. 2017;Vol.65:170–181.

[40] Berdugo Vilches T, Lind F, Rydén M, Thunman H. Experience of more than 1000 h of operation with oxygen carriers and solid biomass at large scale. Applied Energy. 2017;Vol.190:1174–1183.

[41] Haider S, Erans M, Donat F, Duan L, Scott S, Manovic V, et al. Copper-based oxygen carriers supported with alumina/lime for the chemical looping conversion of gaseous fuels. Journal of Energy Chemistry. 2017;Vol.26:891–901.

[42] Xu L, Edland R, Li Z, Leion H, Zhao D, Cai N. Cu-Modified Manganese Ore as an Oxygen Carrier for Chemical Looping Combustion. Energy & Fuels. 2014;Vol.28:7085–7092.
[43] Xu L, Sun H, Li Z, Cai N. Experimental study of copper modified manganese ores as oxygen carriers in a dual fluidized bed reactor. Applied Energy. 2016;Vol.162:940–947.
[44] Lui L. Schematic over macro TGA; 2019.
[45] Lui L, Li Z, Li W, Cai N. The melting characteristics of Vietnamese ilmenite and manganese ores used in chemical looping combustion; 2019.

A

Appendix 1

A.1 TGA experiments

Graphs of the full run of the TGA experiments. On the x-axis, mass ratio (orange) and temperature (blue) are plotted and time is plotted on the y-axis.

A.1.1 FJ with kaolin

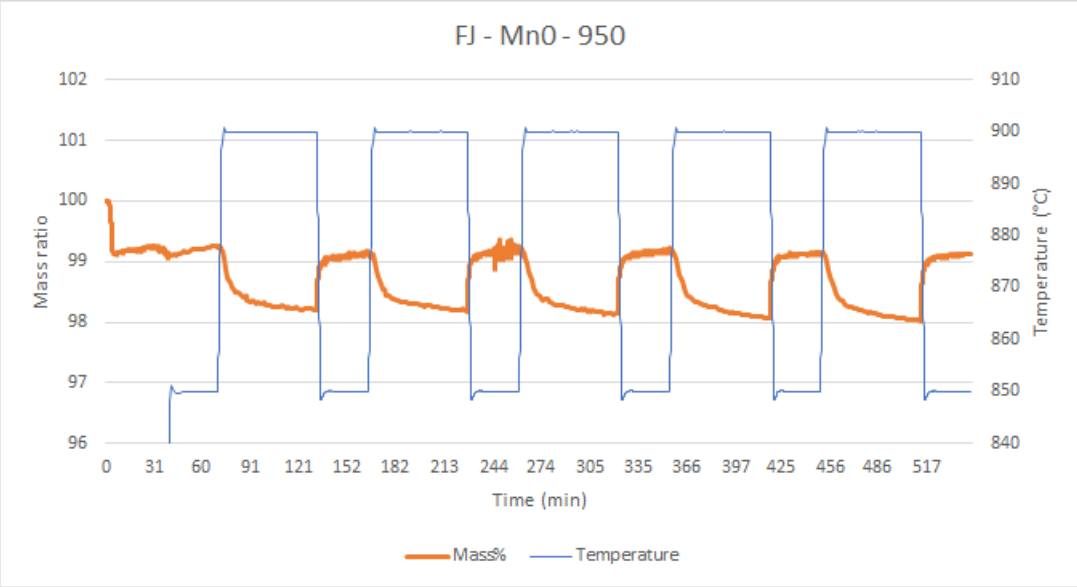

Figure A.1: Full TGA run for FJ-Mn0-950 in N_2 atmosphere.

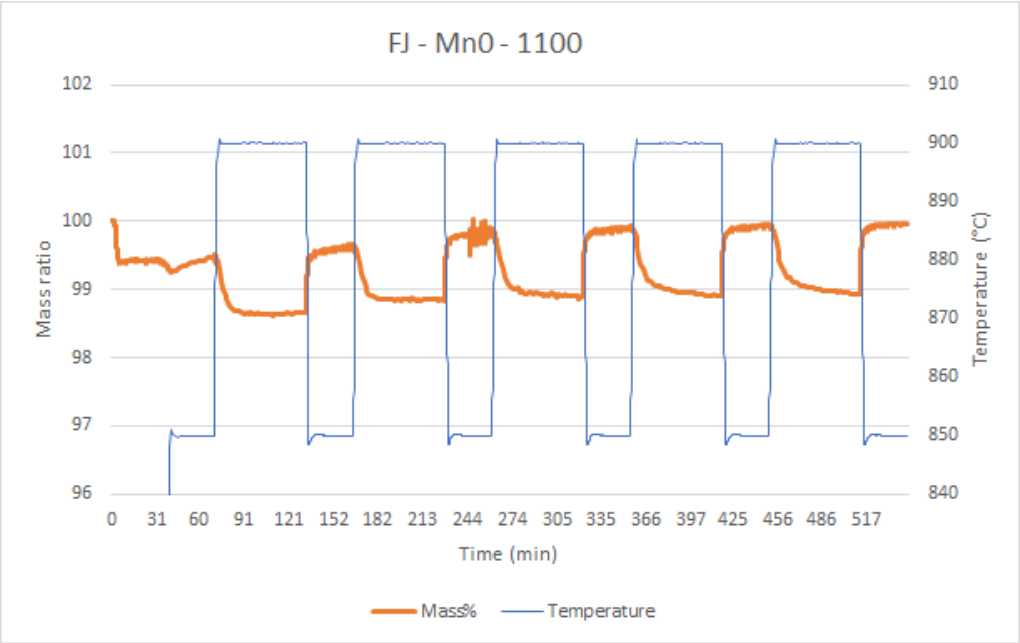

Figure A.2: Full TGA run for FJ-Mn0-1100 in N_2 atmosphere.

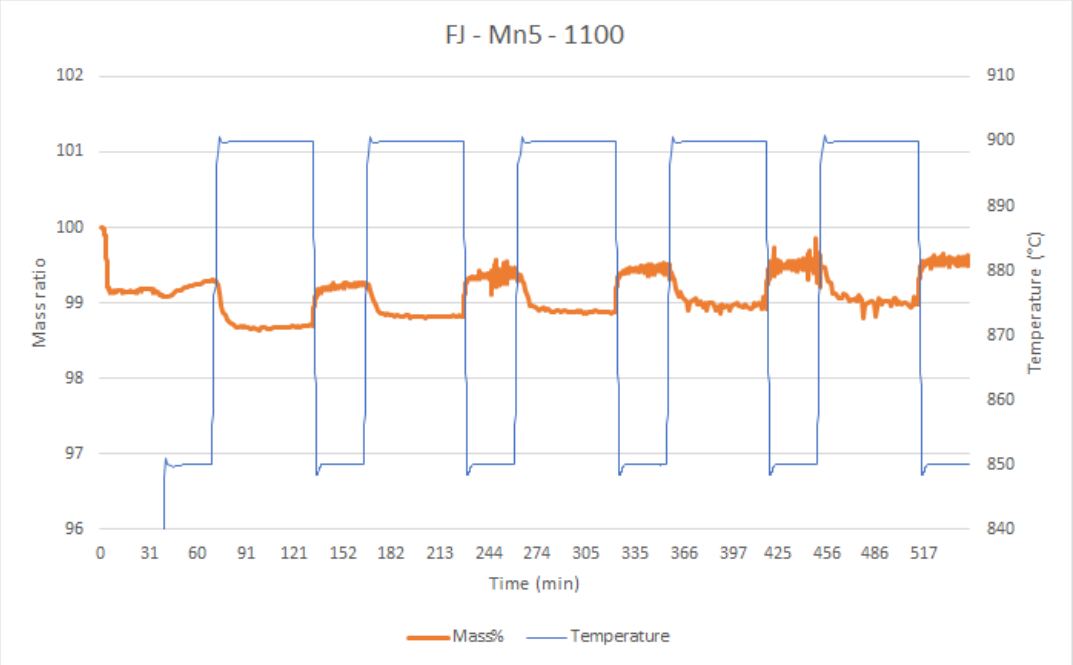

Figure A.3: Full TGA run for FJ-Mn5-1100 in N_2 atmosphere.

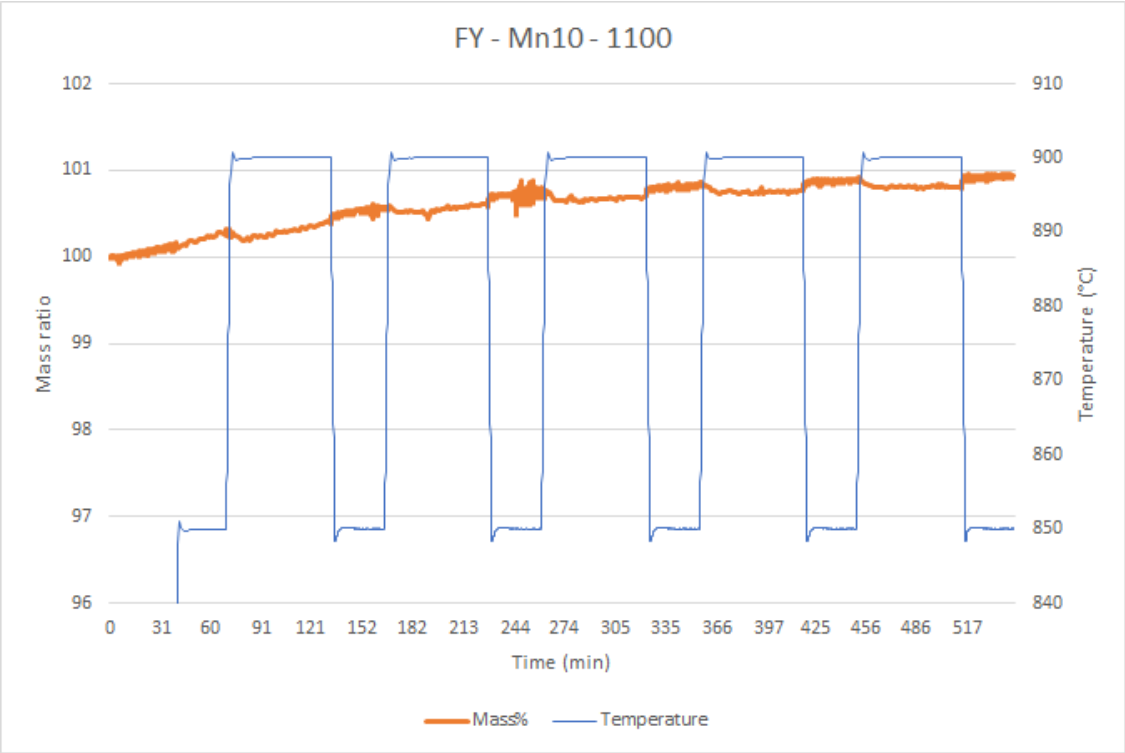

Figure A.4: Full TGA run for FJ-Mn10-1100 in N_2 atmosphere.

A.1.2 LY with kaolin

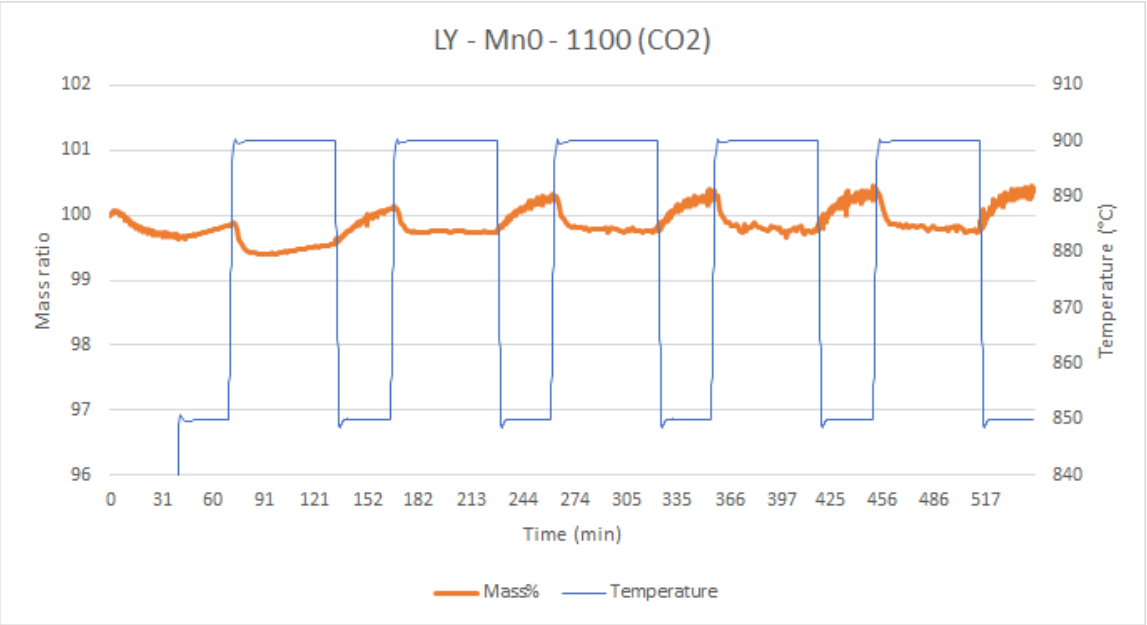

Figure A.5: Full TGA run for LY-Mn0-1100 in CO_2 atmosphere.

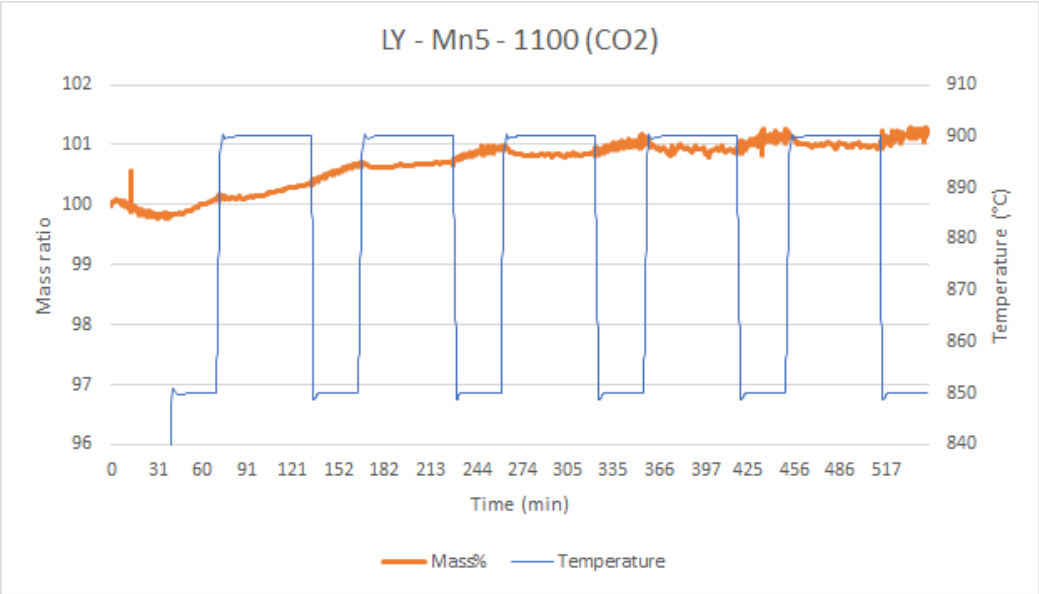

Figure A.6: Full TGA run for LY-Mn5-1100 in CO_2 atmosphere.

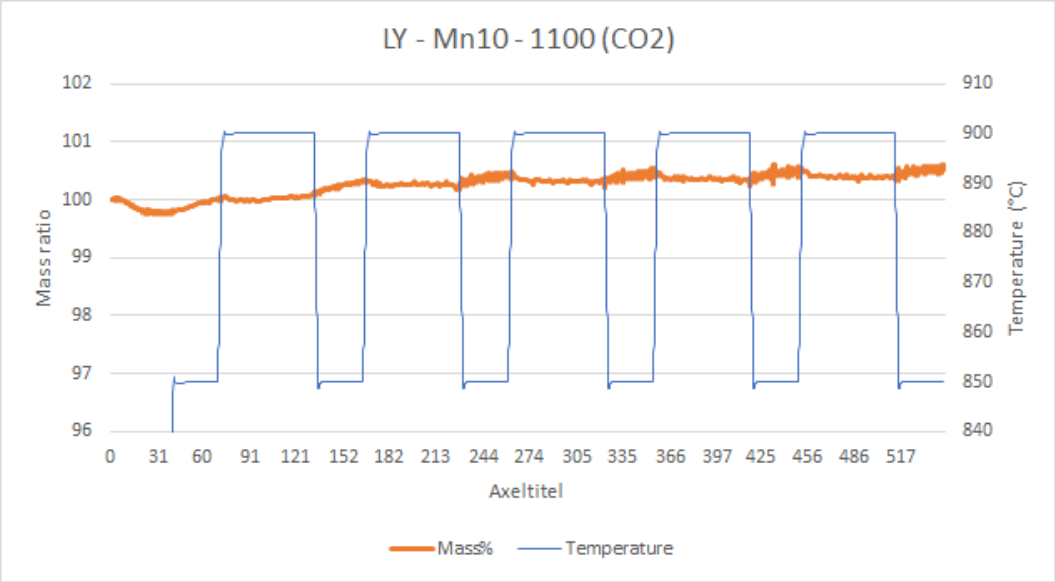

Figure A.7: Full TGA run for LY-Mn10-1100 in CO_2 atmosphere.

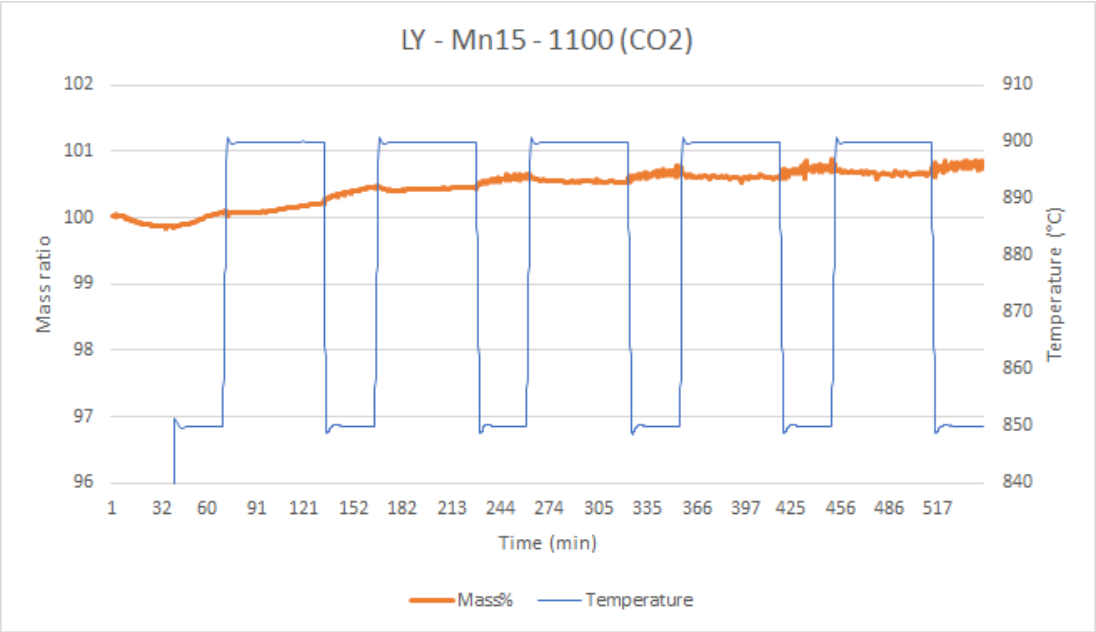

Figure A.8: Full TGA run for LY-Mn15-1100 in CO_2 atmosphere.

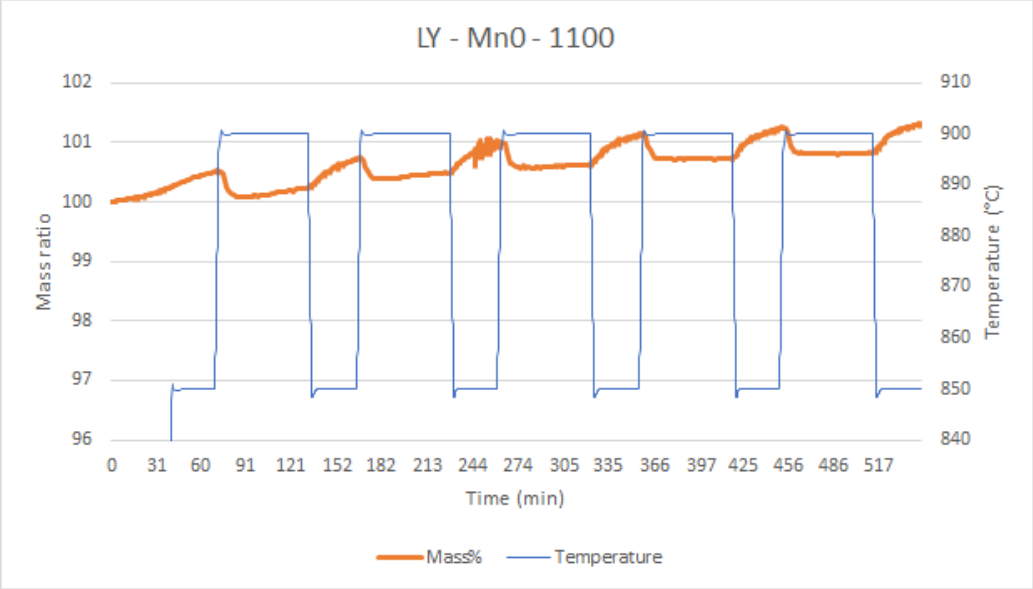

Figure A.9: Full TGA run for LY-Mn0-1100 in N_2 atmosphere.

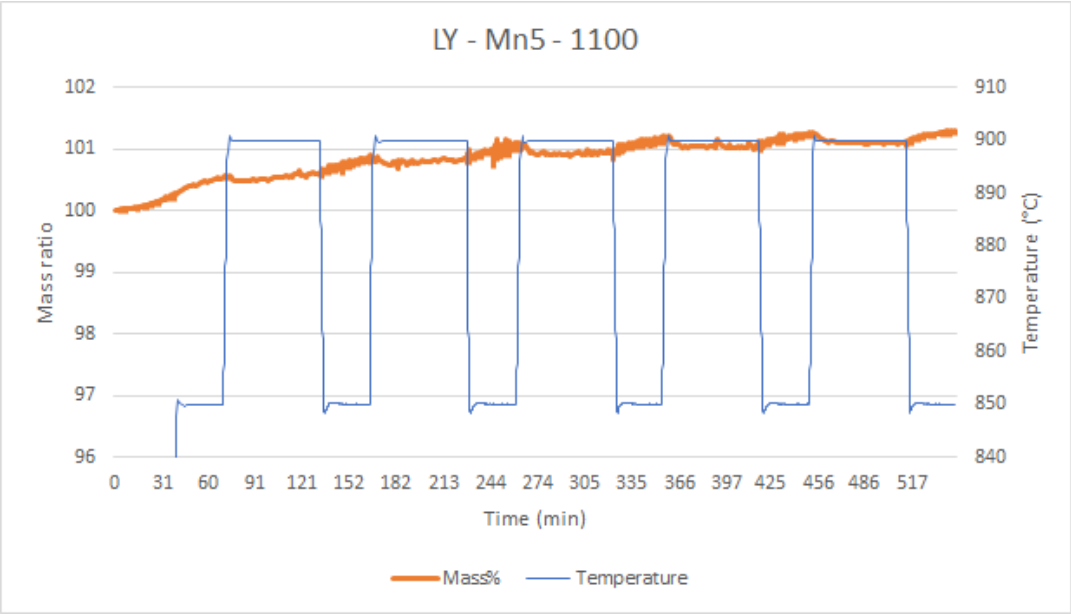

Figure A.10: Full TGA run for LY-Mn5-1100 in N_2 atmosphere.

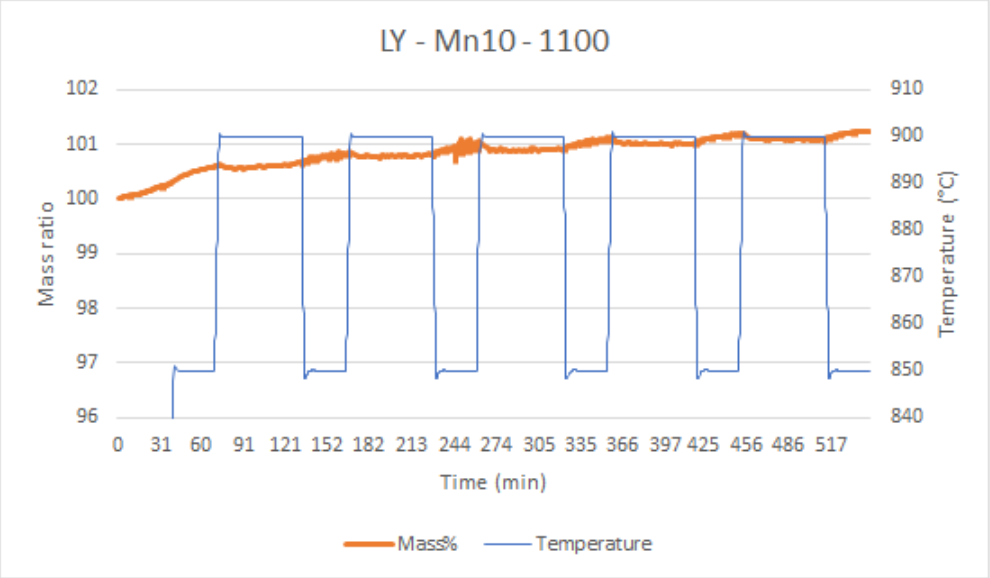

Figure A.11: Full TGA run for LY-Mn10-1100 in N_2 atmosphere.

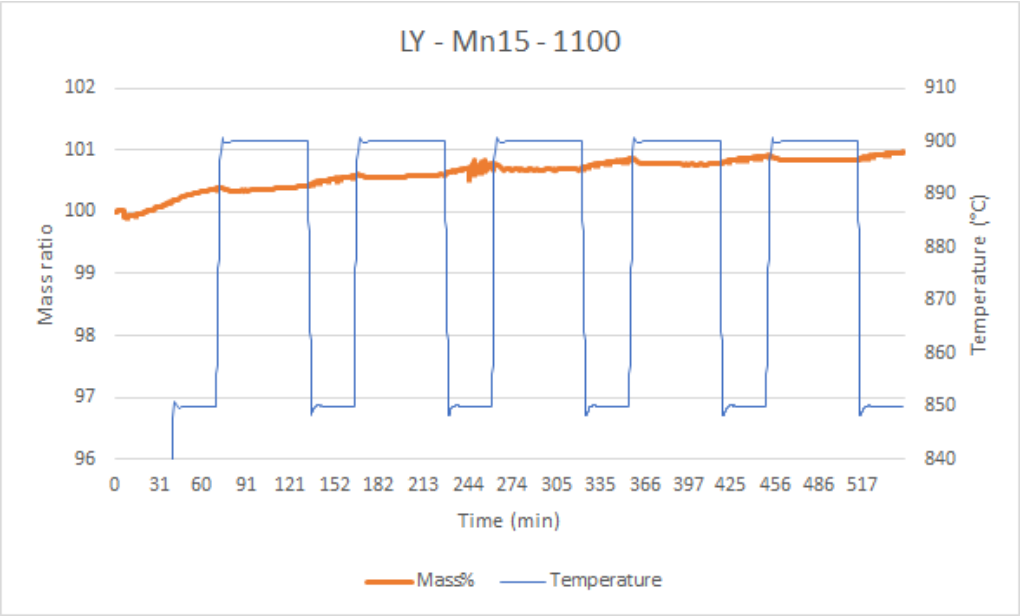

Figure A.12: Full TGA run for LY-Mn15-1100 in N_2 atmosphere.

A.1.3 FJ with copper impregnation

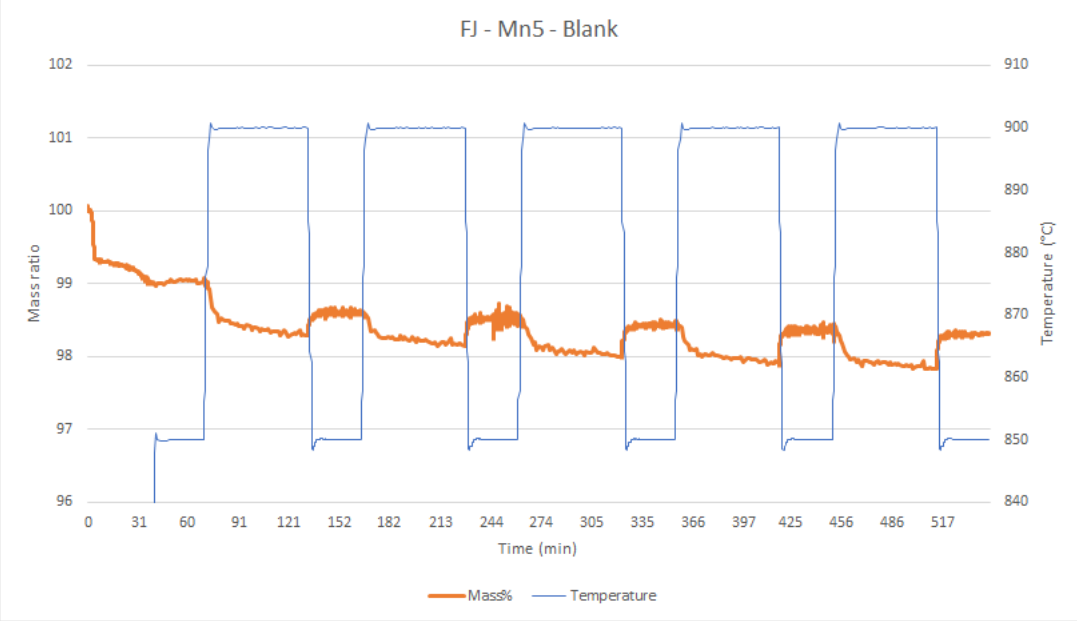

Figure A.13: Full TGA run for FJ-Mn5-1100-blank in N_2 atmosphere.

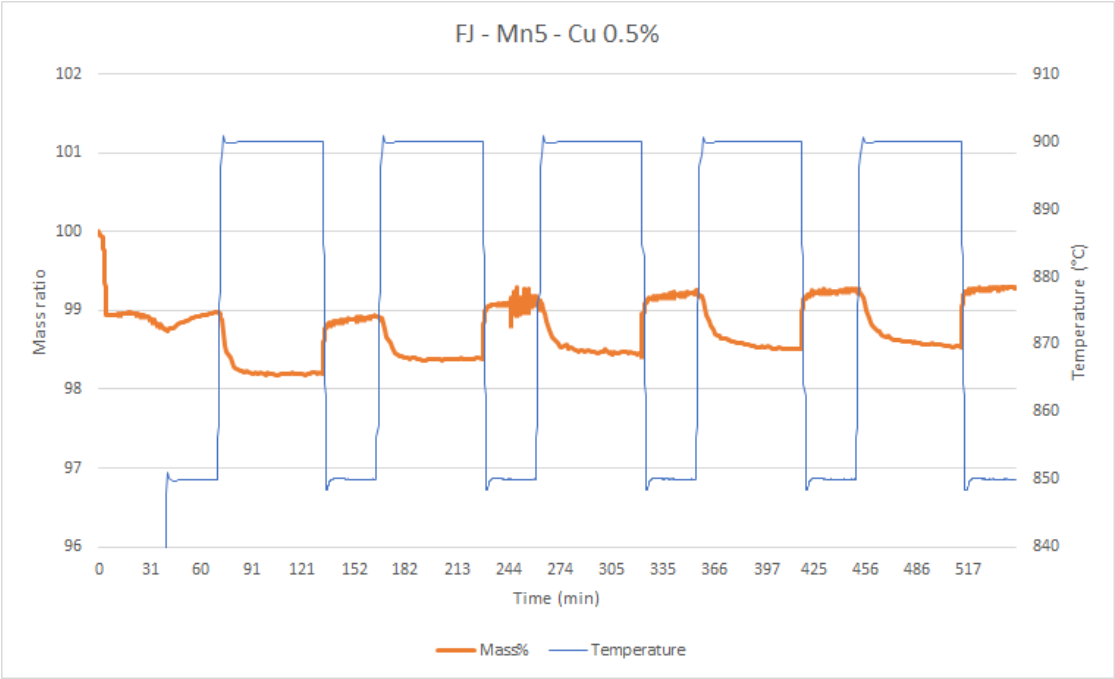

Figure A.14: Full TGA run for FJ-Mn5-1100-Cu0.5 in N_2 atmosphere.

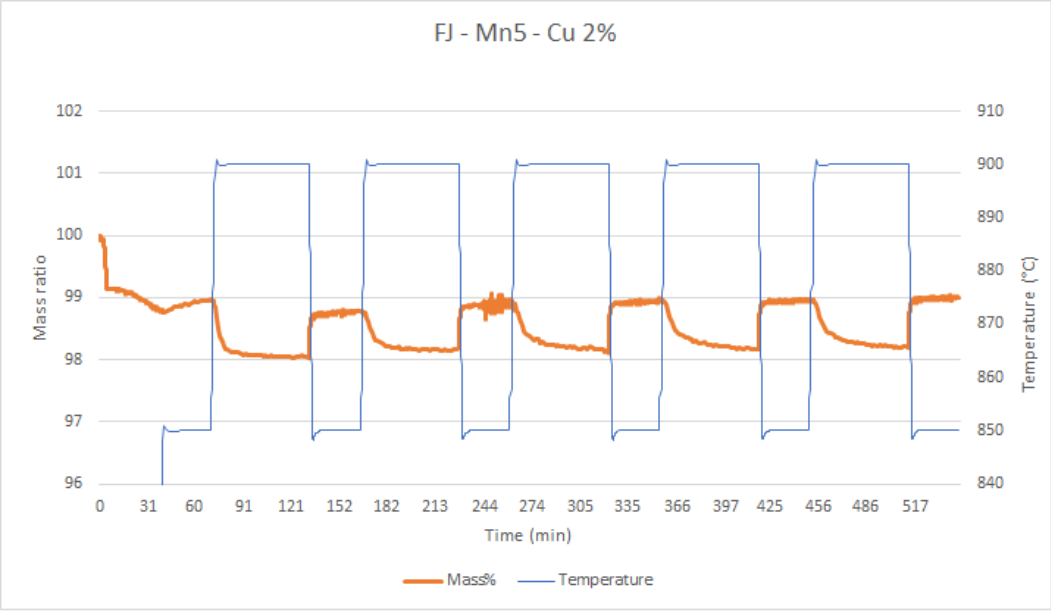

Figure A.15: Full TGA run for FJ-Mn5-1100-Cu2 in N_2 atmosphere.

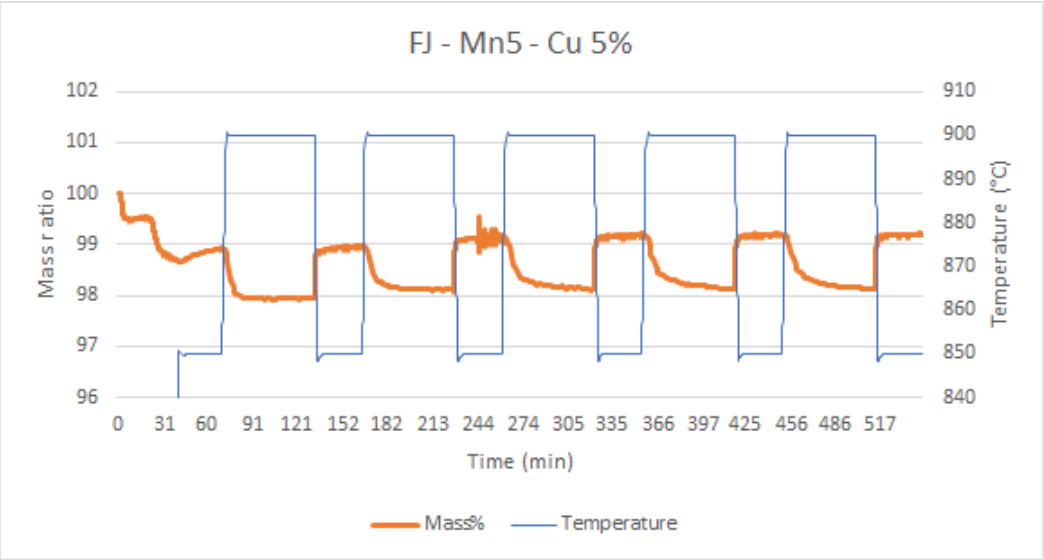

Figure A.16: Full TGA run for FJ-Mn5-1100-Cu5 in N_2 atmosphere.

A.1.4 LY with copper impregnation

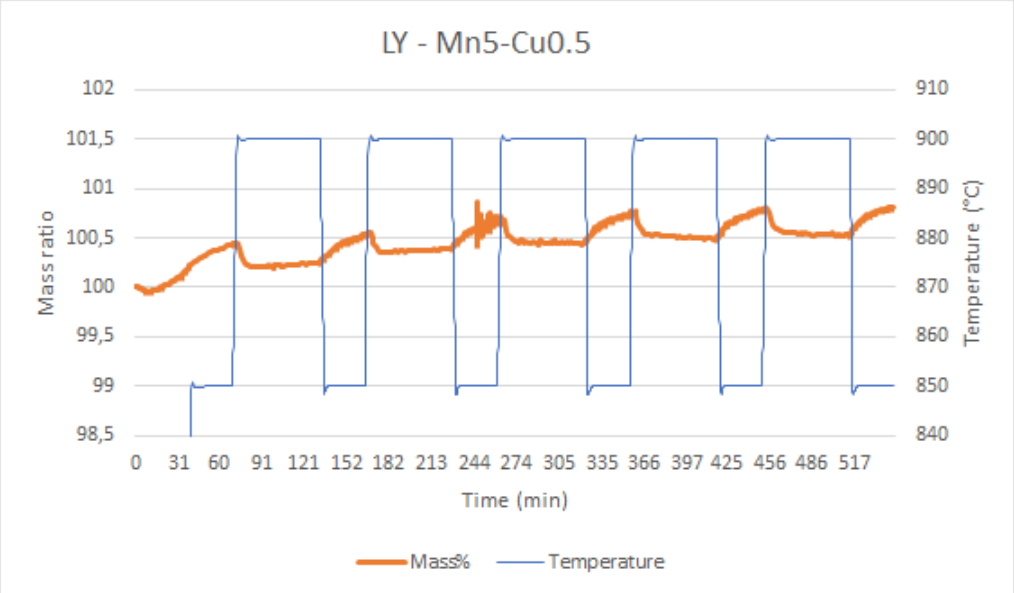

Figure A.17: Full TGA run for LY-Mn5-1100-Cu0.5 in N_2 atmosphere.

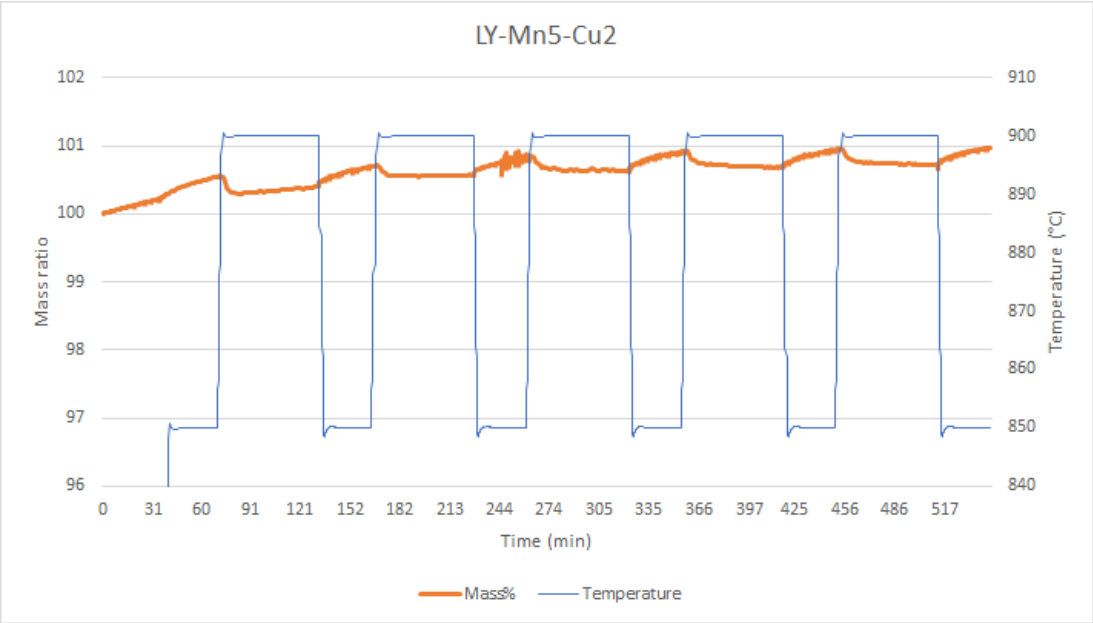

Figure A.18: Full TGA run for LY-Mn5-1100-Cu2 in N_2 atmosphere.

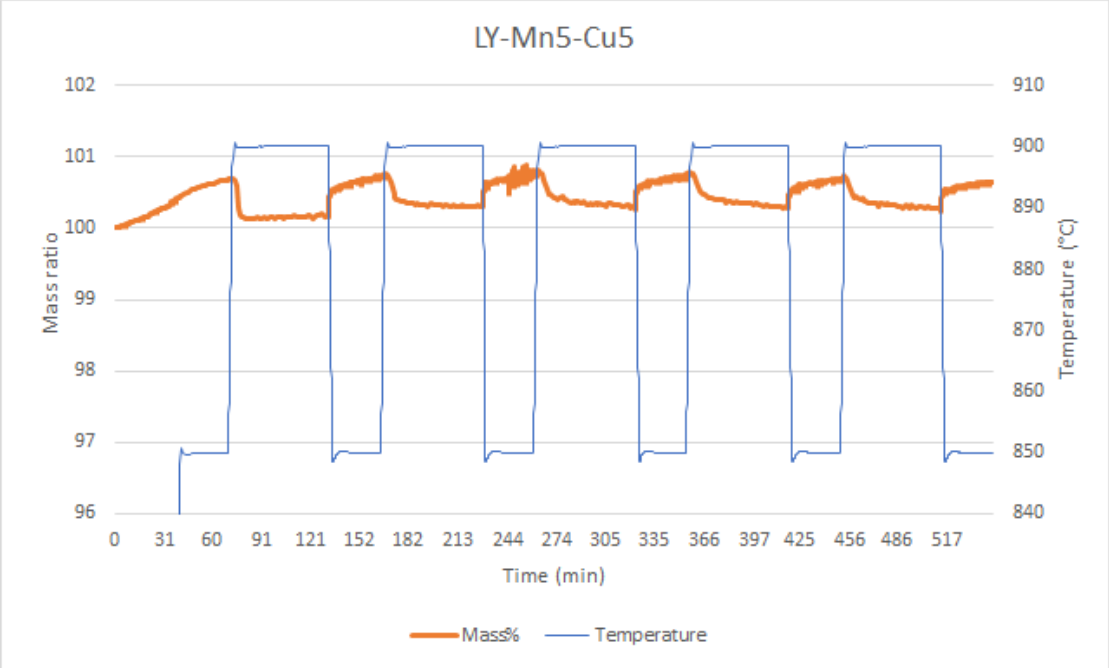

Figure A.19: Full TGA run for LY-Mn5-1100-Cu5 in N_2 atmosphere.

A.1.5 Post macro TGA

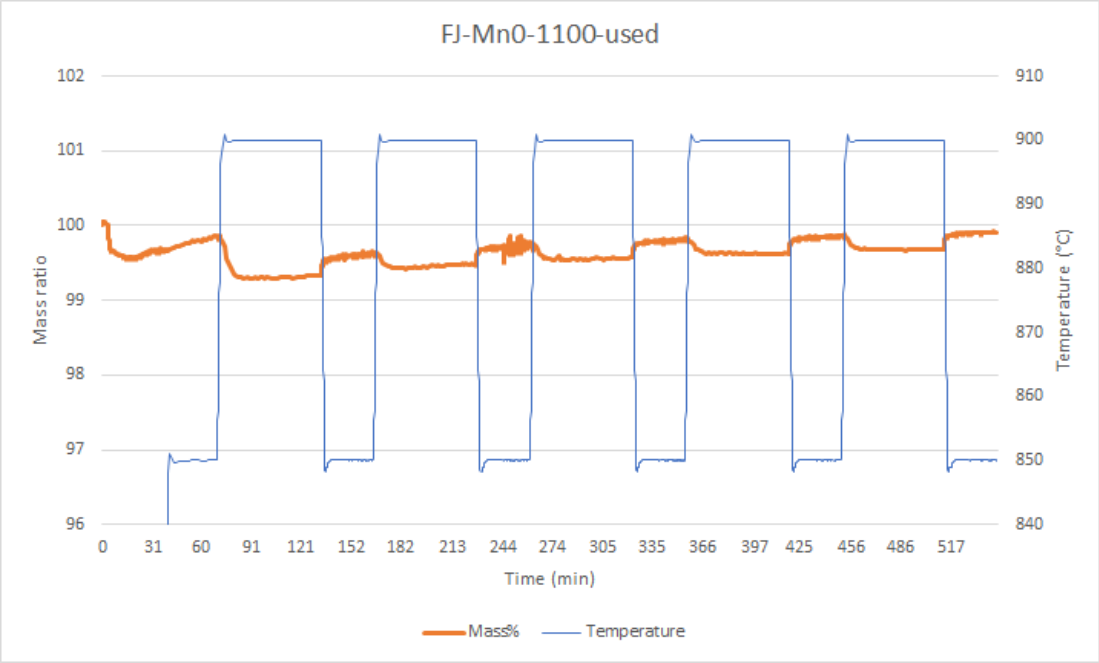

Figure A.20: Full TGA run for FJ-Mn0-1100 in N_2 atmosphere after macro TGA analysis.

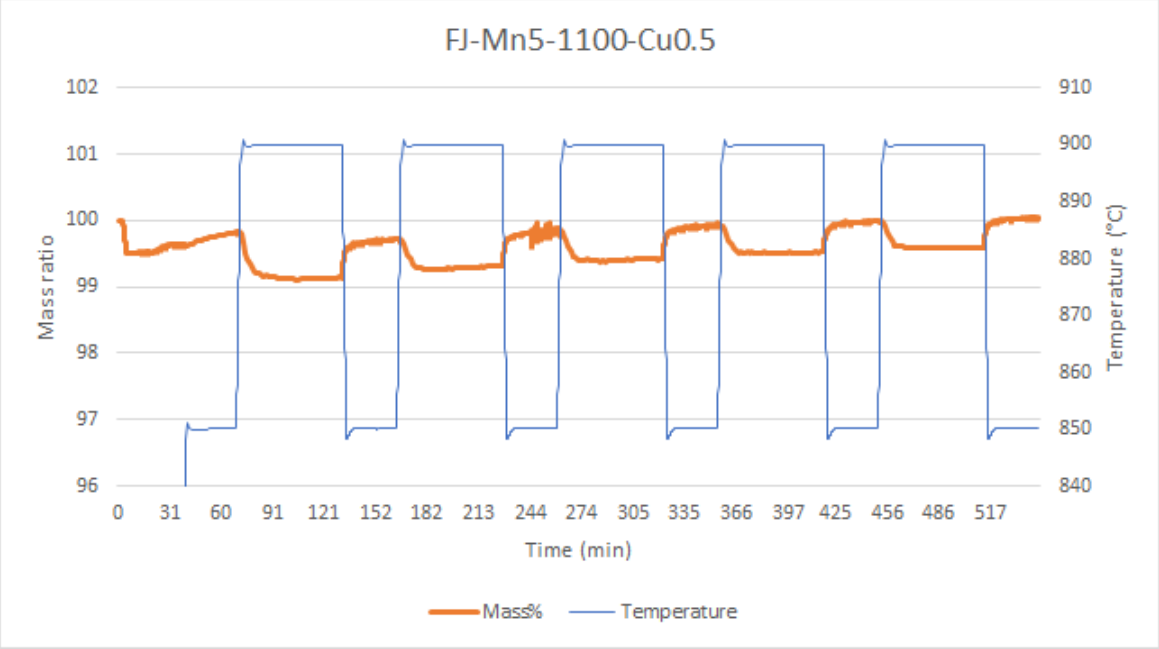

Figure A.21: Full TGA run for FJ-Mn5-1100-Cu0.5 in N_2 atmosphere after macro TGA analysis.

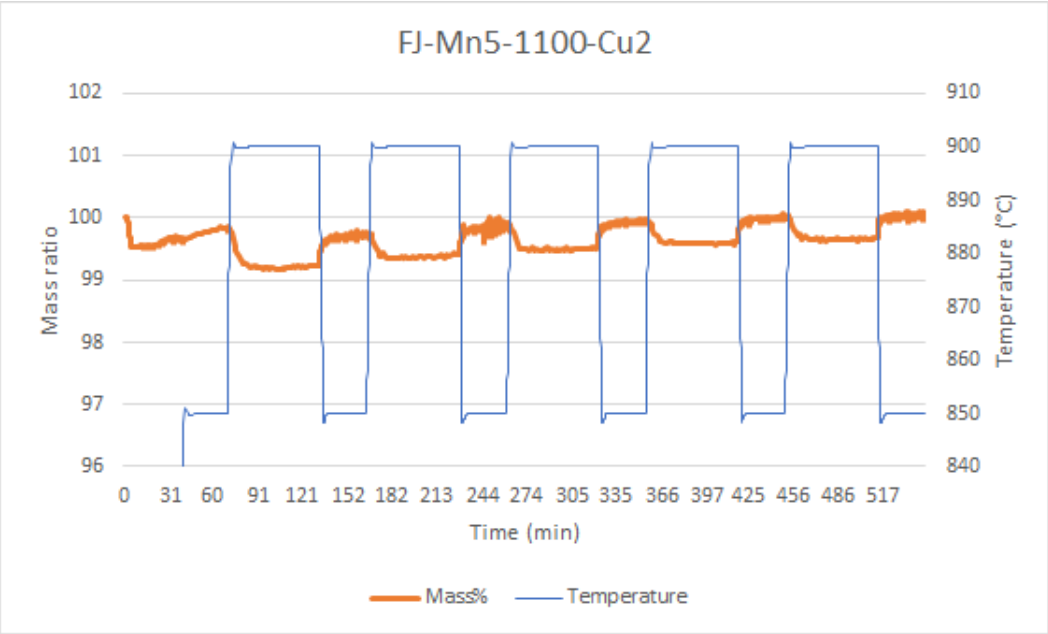

Figure A.22: Full TGA run for FJ-Mn5-1100-Cu2-used in N_2 atmosphere atmosphere after macro TGA analysis.

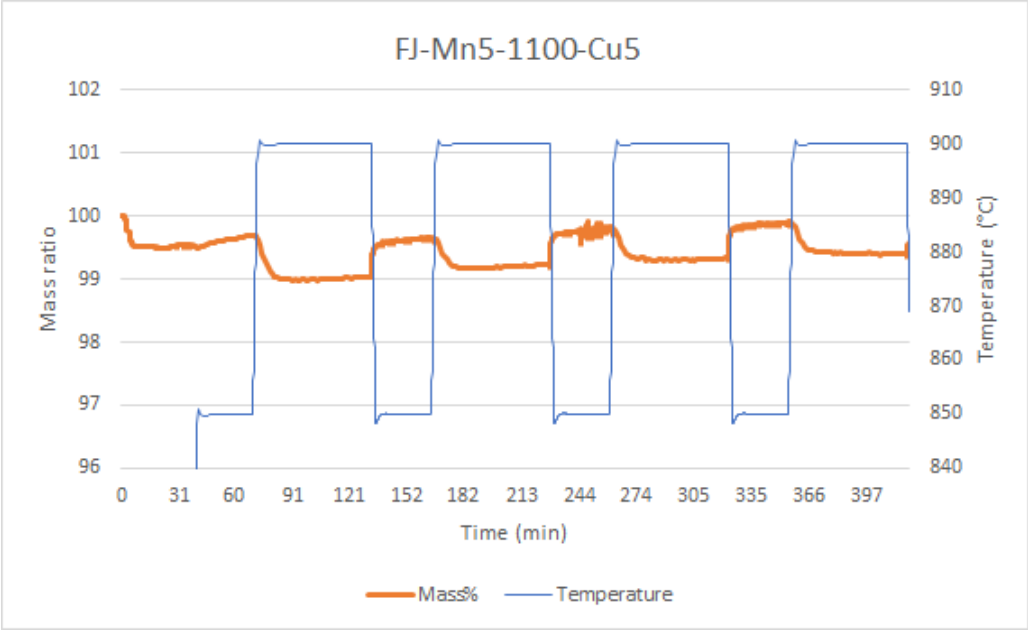

Figure A.23: Full TGA run for FJ-Mn5-1100-Cu5 in N_2 atmosphere after macro TGA analysis.

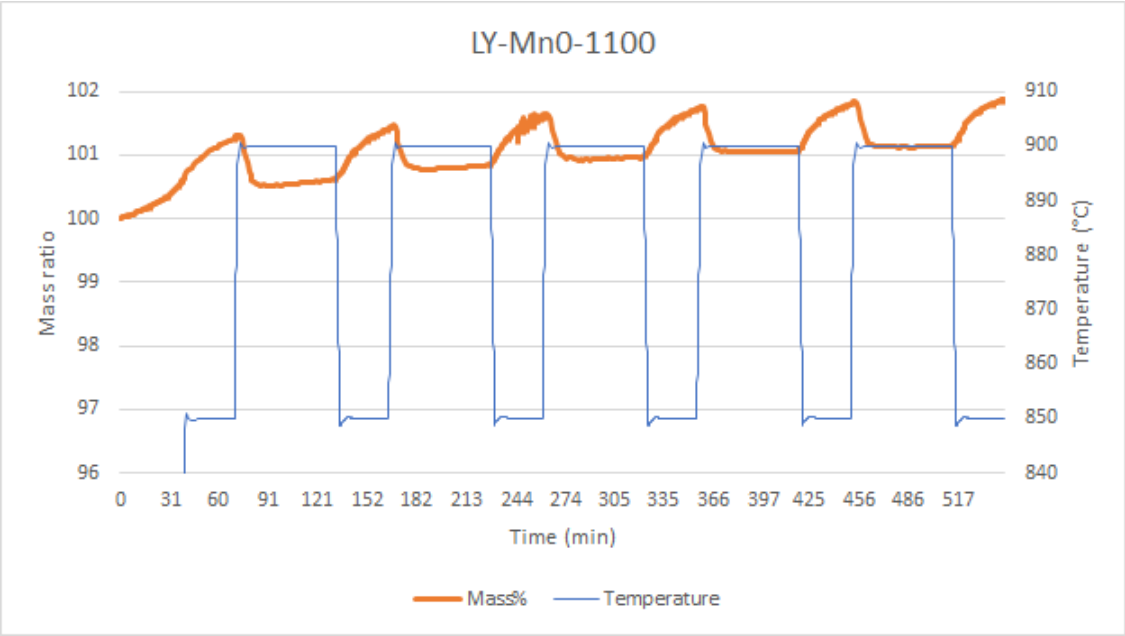

Figure A.24: Full TGA run for LY-Mn0-1100 in N_2 atmosphere after macro TGA analysis.

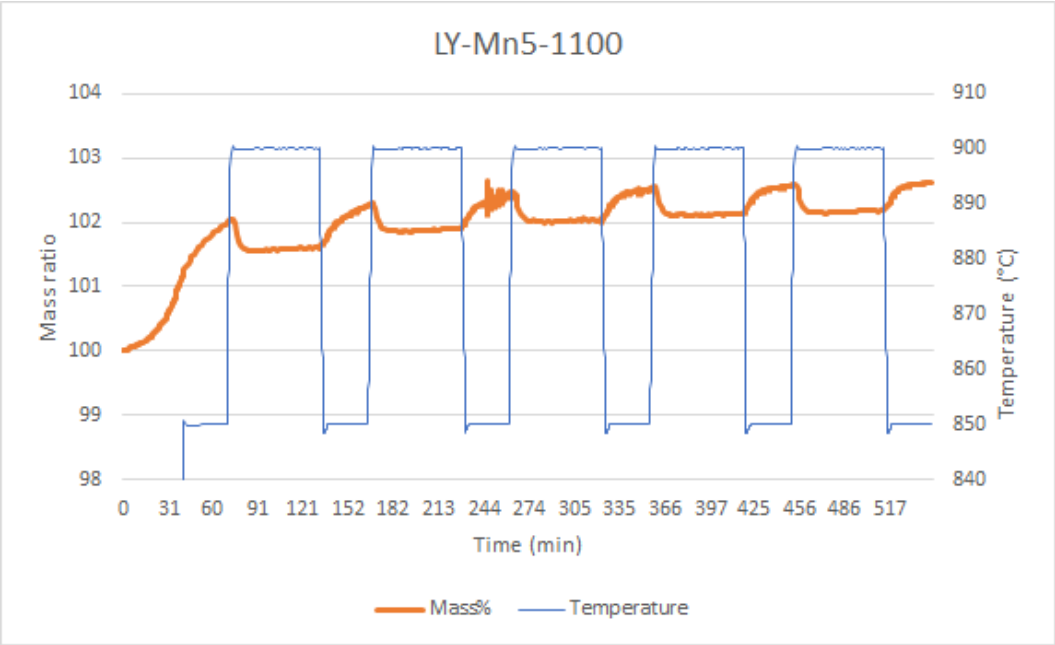

Figure A.25: Full TGA run for LY-Mn5-1100 in N_2 atmosphere after macro TGA analysis.

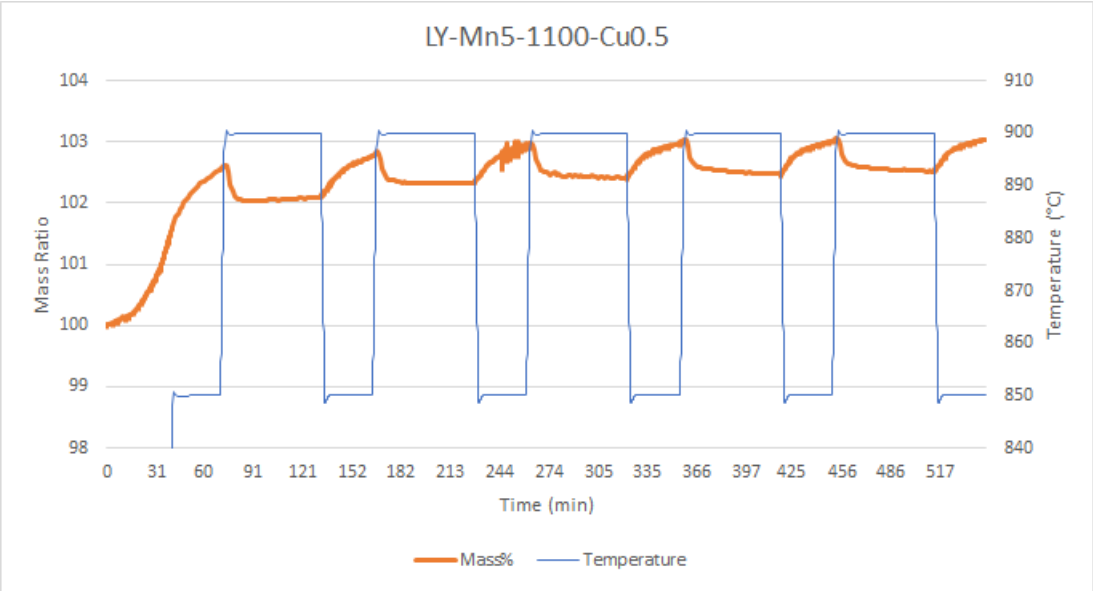

Figure A.26: Full TGA run for LY-Mn5-1100-Cu0.5 in N_2 atmosphere after macro TGA analysis.

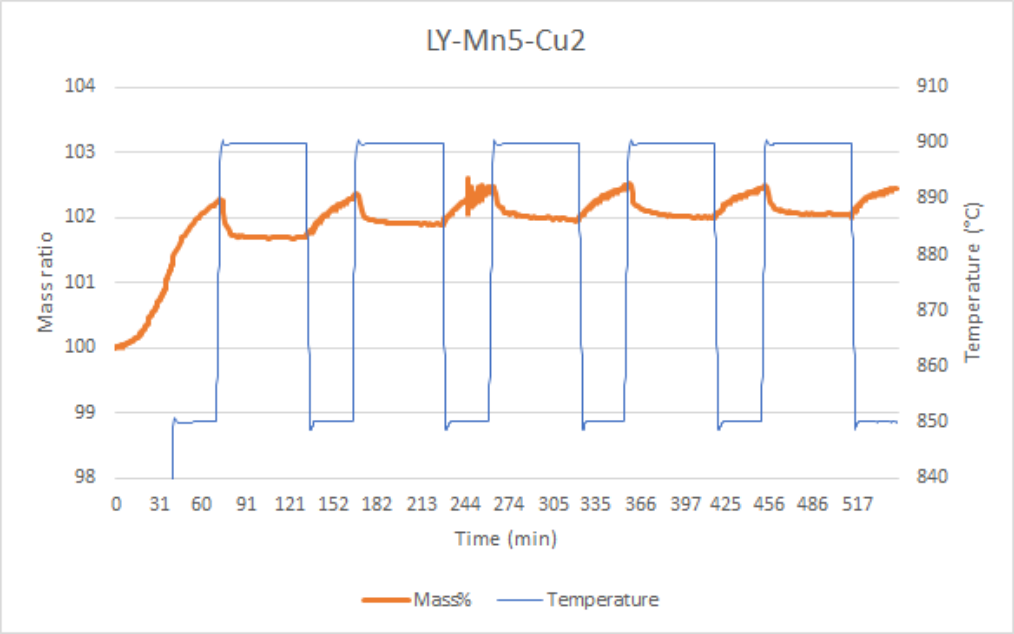

Figure A.27: Full TGA run for LY-Mn5-1100-Cu2 in N_2 atmosphere after macro TGA analysis.

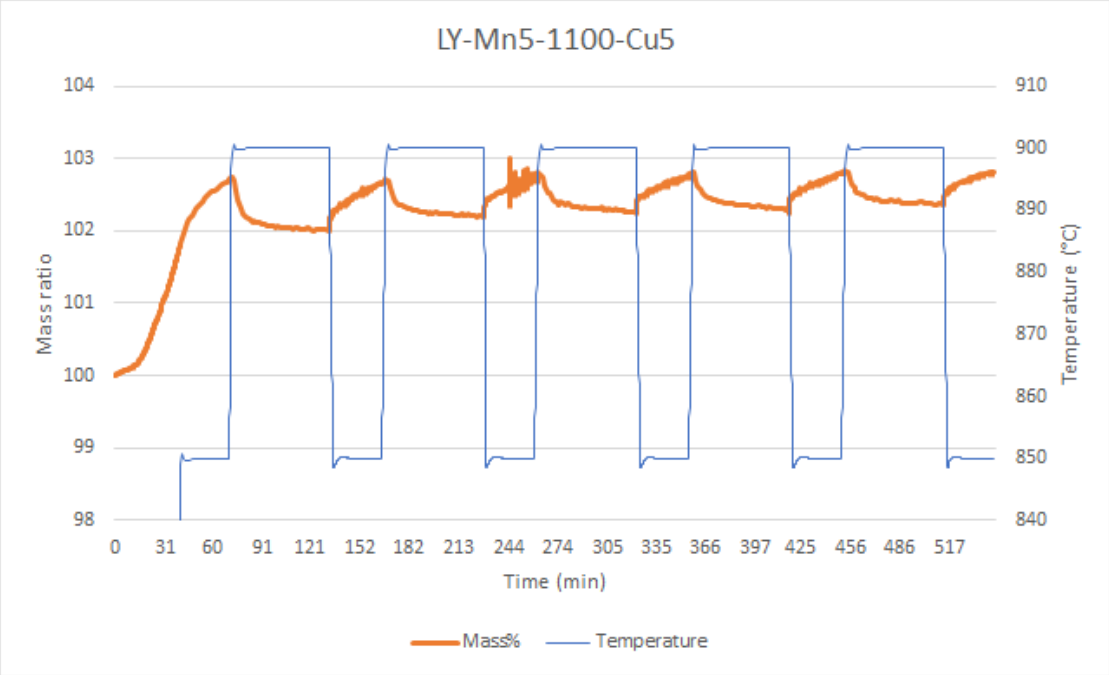

Figure A.28: Full TGA run for LY-Mn5-1100-Cu5 in N_2 atmosphere after macro TGA analysis.

A.1.6 Temperature investigation

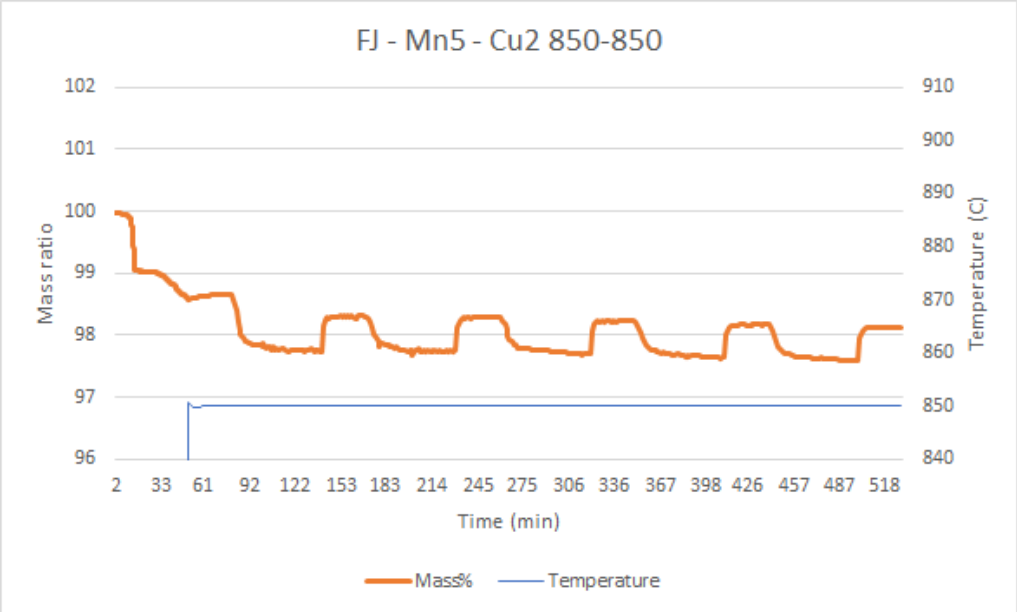

Figure A.29: Full TGA run for FJ-Mn5-1100-Cu2 in N_2 atmosphere with 850-850 temperature profile.

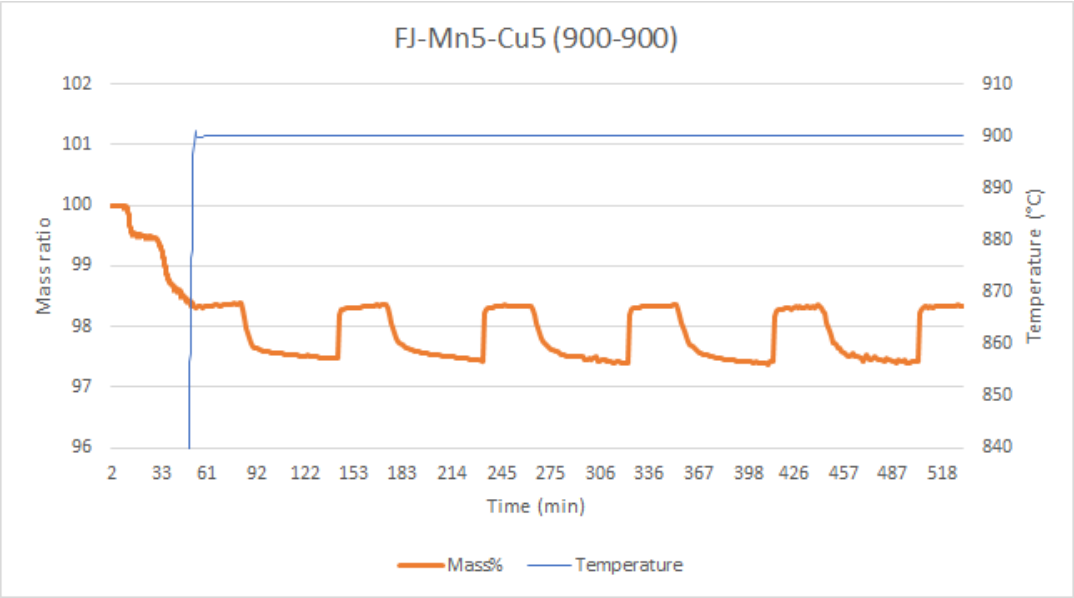

Figure A.30: Full TGA run for FJ-Mn5-1100-Cu5 in N_2 atmosphere with 900-900 temperature profile.

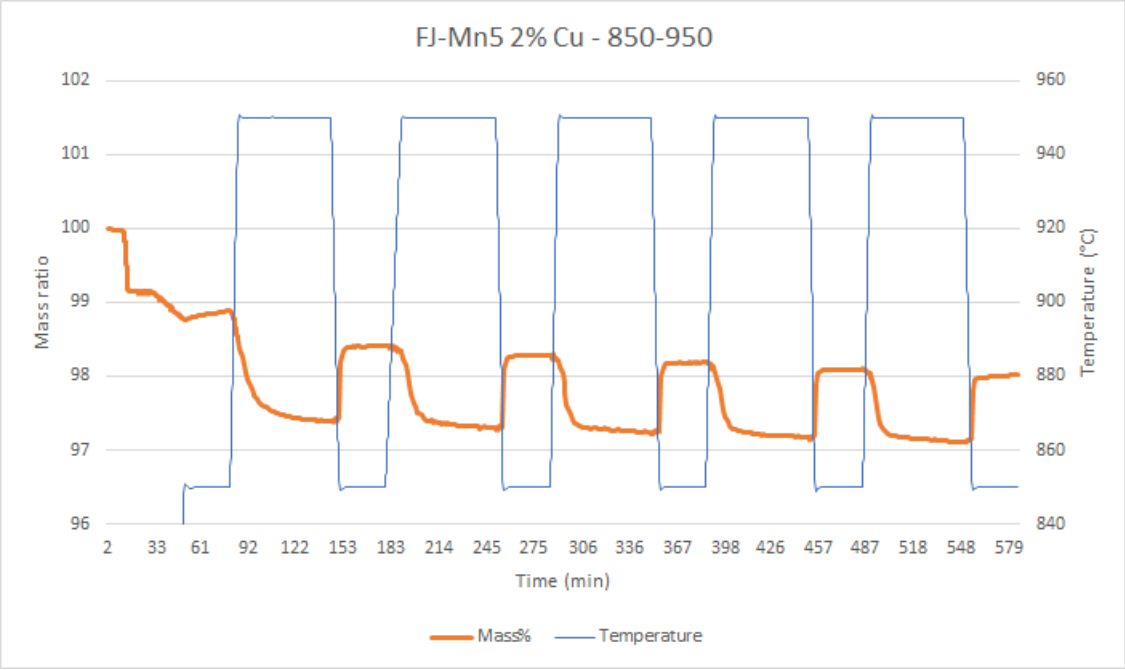

Figure A.31: Full TGA run for FJ-Mn5-1100-Cu2 in N_2 atmosphere with 850-950 temperature profile.

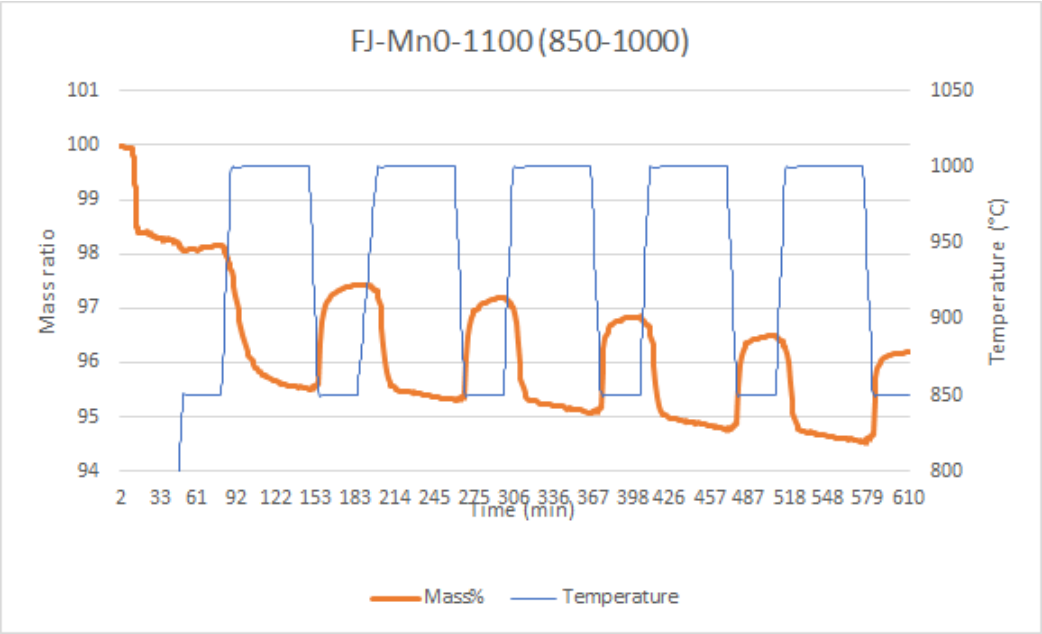

Figure A.32: Full TGA run for FJ-Mn0-1100 in N_2 atmosphere with 850-1000 temperature profile.

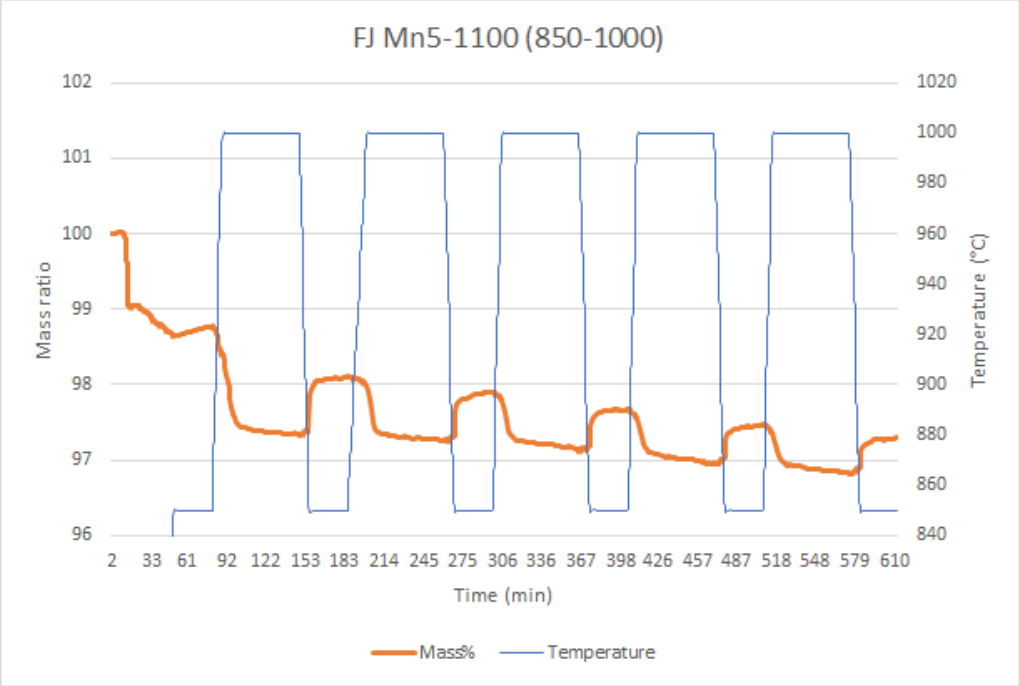

Figure A.33: Full TGA run for FJ-Mn5-1100 in N_2 atmosphere with 850-1000 temperature profile.

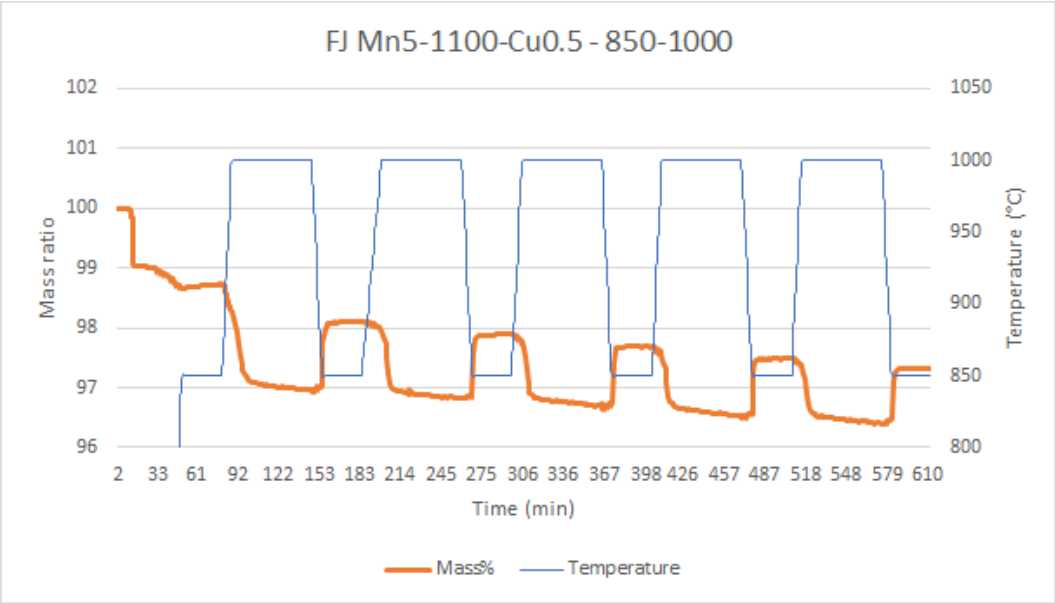

Figure A.34: Full TGA run for FJ-Mn5-1100-Cu0.5 in N_2 atmosphere with 850-1000 temperature profile.

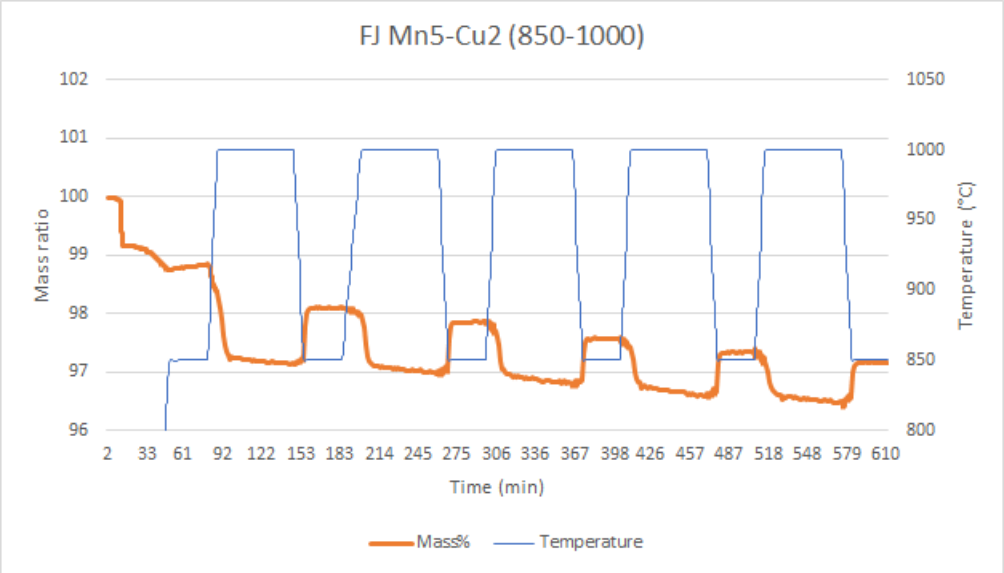

Figure A.35: Full TGA run for FJ-Mn5-1100-Cu2 in N_2 atmosphere with 850-1000 temperature profile.